
# CAVITY COUPLED AERORAMP INJECTOR COMBUSTION STUDY

THESIS

Dell T. Olmstead, Captain, USAF

AFIT/GAE/ENY/09-J03

**DEPARTMENT OF THE AIR FORCE**
**AIR UNIVERSITY**

***AIR FORCE INSTITUTE OF TECHNOLOGY***

**Wright-Patterson Air Force Base, Ohio**

The views expressed in this thesis are those of the author and do not reflect the official policy or position of the United States Air Force, Department of Defense, or the United States Government.

AFIT/GAE/ENY/09-J03

# CAVITY COUPLED AERORAMP INJECTOR COMBUSTION STUDY

THESIS

Presented to the Faculty

Department of Aeronautics and Astronautics

Graduate School of Engineering and Management

Air Force Institute of Technology

Air University

Air Education and Training Command

In Partial Fulfillment of the Requirements for the

Degree of Master of Science in Aeronautical Engineering

Dell T. Olmstead

Captain, USAF

June 2009

AFIT/GAE/ENY/09-J03

# CAVITY COUPLED AERORAMP INJECTOR COMBUSTION STUDY

Dell T. Olmstead

Captain, USAF

Approved:

/signed/ _____
LtCol Richard D. Branam, USAF (Chairman) date

/signed/ _____
Dr. Mark R. Gruber (Member) date

/signed/ _____
Dr. Paul I. King (Member) date

# Abstract

The difficulties with fueling of supersonic combustion ramjet engines with hydrocarbon based fuels presents many challenges that are currently being tackled by the Air Force Research Lab Propulsion Directorate Aerospace Propulsion Division. As the scramjet engine designs are scaled up, the need for a better solution to supersonic mixing has led to the development of many different styles of fuel injection. An aerodynamic ramp injector has been shown to have a quantitative improvement over a physical ramp while still achieving desirable mixing characteristics. Little quantitative data is available on the performance of aerodynamic ramp injectors in a cavity-coupled scramjet flowpath, especially relative to round injectors. The objectives for this research was quantifying the performance and operability implications of replacing four 15 degree round injectors with four arrays of improved aeroramp injectors. Ignition limits and pre-combustion shock position were used to define the operability differences while combustion efficiency was the primary metric used for performance comparisons. These parameters were determined by operating a scramjet combustor in dual-mode operation over the range of Mach numbers expected during scramjet takeover from a boost vehicle. Performance and operability data was derived from data taken determining the ignition limits, the wall static pressures, temperature measurements, and thrust stand loading. It was determined that the operability reduces significantly for the aeroramp injector, but the performance is virtually identical to the round injectors. The aeroramp injector indicated improved near-field combustion indicating the potential for better performance in higher Mach number flow to include full scramjet mode.

# Acknowledgements

I would like to thank my advisor, LtCol Richard Branam for his guidance in this research. I greatly appreciate the assistance and mentoring provided by my sponsor, Dr. Mark Gruber who has devoted many hours to answering my numerous questions on both this research and throughout my tenure at AFRL. My thanks go out to the members of the AFRL/RZAS in-house test team including Dr. Skip Williams, Dr. Steven Lin, Steve Enneking, Matt Streby, Tim Bulcher, 1st Lt MacKenzie Collatz, and 2nd Lt John Heaton, all who spent many late nights running experiments with me and have been extremely helpful in my research. I would also like to thank Dr. John Tam for his assistance in reducing and analyzing the mountains of data. I greatly appreciate the educational opportunity afforded me by the Air Force Research Laboratory Propulsion Directorate in conducting this research. Finally, I would like to thank my wife and kids for their loving support and patience during this challenging process. I could not be here without their help.

# Table of Contents

Page

# List of Figures

Page

# List of Tables

Page

# List of Symbols

Symbol

| | |
|---|---|
| $A_{base}$ | Test article base area ($in^2$) |
| $A_5$ | Combustor exit area ($in^2$) |
| F | Thrust stand force (lbf) |
| $H_5$ | Combustor exit enthalpy (Btu/lbm) |
| $H_a$ | Vitiator exit air enthalpy (Btu/lbm) |
| $H_f$ | Combustor fuel enthalpy (Btu/lbm) |
| I-1 | Injector 1 |
| I-2 | Injector 2 |
| I-5 | Injector 5 |
| I-6 | Injector 6 |
| $I_{sp}$ | Specific impulse |
| $P_{amb}$ | Ambient pressure (psi) |
| $P_{base}$ | Test article base pressure (psi) |
| $P_5$ | Combustor exit pressure (psi) |
| Q | Dynamic pressure (psf) |
| $R_u$ | Universal gas constant $\left(1545.4\,\frac{ft*lbf}{lbmol*R}\right)$ |
| $St_5$ | Stream thrust at combustor exit (lbf) |
| $T_5$ | Average combustor exit temperature (R) |
| $U_5$ | Combustor exit velocity (ft/s) |
| $W_a$ | Air mass flow rate (lbm/s) |
| $W_f$ | Fuel mass flow rate (lbm/s) |
| $W_5$ | Combustor exit mass flow rate (lbm/s) |

$Y_{froz}$ Mass fraction of fuel at combustor exit

$\alpha_{mix}$ Fuel mixing coefficient

$\eta_c$ Combustion efficiency

$\rho_5$ Combustor exit density ($lbm/in^3$)

$\Phi$ Equivalence ratio

# List of Abbreviations

| Abbreviation | |
|---|---|
| Aeroramp | Aerodynamic Ramp Injector |
| AFIT | Air Force Institute of Technology |
| AFRL | Air Force Research Laboratory |
| CFD | Computational Fluid Dynamics |
| DMRJ | Dual Mode Ramjet |
| DMSJ | Dual Mode Scramjet |
| ICBM | Intercontinental Ballistic Missile |
| LASER | Light Amplification by Stimulate Emission of Radiation |
| L/D | Ratio of Length of Cavity to Depth of Cavity |
| L/H | Ratio of Length of Isolator to Throat Height |
| MW | Molecular Weight |
| PLIF | Planar Laser Induce Fluorescence |
| RC-18 | Propulsion Research Cell 18 at Wright-Patterson Air Force Base |
| Scramjet | Supersonic Combustion Ramjet |
| TDLAS | Tunable Diode Laser Absorption Spectroscopy |
| USAF | United States Air Force |
| X-51A | Scramjet Engine Demonstrator |

# CAVITY COUPLED AERORAMP INJECTOR COMBUSTION STUDY

## I. Introduction

### I.1 Motivation

The ability to strike targets at a long distance quickly has been a goal of the United States Air Force since its inception. Since 1947, technology has advanced such that the definition of long distance includes the entire world and high speed is bounded only by the speed of light. While the USAF can currently engage targets almost anywhere on the world with its fleet of Intercontinental Ballistic Missiles (ICBMs), they cannot be retargeted in flight due to the ballistic trajectory. Cruise missiles can be retargeted, but there is no system currently fielded that can fly high enough, fast enough, and far enough to allow the delivery vehicle to stay outside the threat envelope while engaging a high value target in a matter of minutes.

One potential propulsion technology to enable this capability is the supersonic combustion ramjet (scramjet). A scramjet powered missile flying at Mach 6.5 at almost 100,000 feet can travel over 350 miles in five minutes and is virtually unstoppable by current anti-air systems. This would allow the strike aircraft carrying it to be much further away than current weapons while allowing the target to be engaged more quickly. This standoff increase would provide an exponential benefit to the mission because the ground fire suppression systems and associated support aircraft would not be needed thus removing many of the sorties required to engage a target. [(1)]

To date there have been only two flights of air breathing scramjet engines, both burning hydrogen and accumulating only a handful of seconds of flight. The United

States Air Force Research Laboratory (AFRL) has developed the first fuel cooled, flight weight, hydrocarbon fueled, dual-mode supersonic combustion ramjet (DMSJ), which is being flown in the X-51A demonstrator vehicle in the fall of 2009. [2] The successful flight will provide a launch point for using hypersonic air breathing propulsion for various applications such as prompt global strike and affordable, responsive space access. There are many components that must be improved to make supersonic combustors viable for a fielded system both for the current engine and especially for the larger engines necessary for anything larger than a small cruise missile. [3]

The components to be assessed in this research are primarily the fuel injectors, with attention paid to how they interact with the flame holder and ignition systems. Current fuel injection is from multiple sets of single-hole injectors at various axial locations, with variations including physical struts to improve the mixing. [4] These approaches are not ideal as the single hole injectors do not mix quickly enough and do not penetrate far enough to get sufficient fuel mixing in a large scramjet. The physical struts allow for much improved mixing and combustion, but with extremely high drag and fuel cooling requirements. Aerodynamic ramps utilize the injection of the fuel to create a swirling fuel plume that mixes much faster and is expected to penetrate further into the flow than a conventional angled round fuel injector. [5]

## I.2 Problem Statement

Current techniques to achieve better mixing of the fuel in a high speed combustor either have poor mixing requiring a long combustor or have intrusive struts; both exaggerate already demanding cooling requirements. An aerodynamic ramp is intended

to utilize the flow of the fuel injector to provide the improved mixing of a strutted or ramp injector without the cooling or efficiency losses incumbent upon intrusive devices in supersonic flow. A sketch of a standard injector, an aeroramp, physical ramp, and strut can be seen in Figure 1.

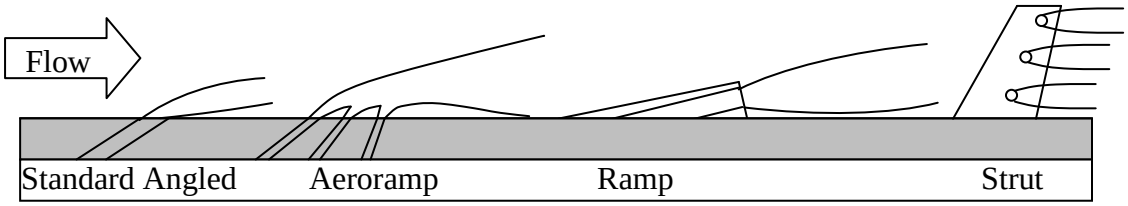


**Figure 1: Standard angle, aeroramp, ramp, and strut injectors**

To date, many of the studies of aeroramp injectors have focused on coupling with a plasma torch igniter. [6] This type of igniter may not be the best technique to light a supersonic combustor and is not indicative of the desired sustained combustion condition. Very little assessment has been done using the aeroramp injector style with a cavity flame holder. The cavity flameholder is a feature likely to be present in some form on any near-term design whether on the wall or as a part of a strut. Tests coupling the aeroramp injector with a cavity were not in a full near steady-state combustion environment with thrust data. [3]

## I.3 Research Objectives

The objectives of this research were to first determine the operability of the direct connect combustor due to the more rapid mixing of the aeroramp injector A useful parameter is the change in shock train position between configurations. The second objective is to determine the effects of the aeroramp configuration on the performance and efficiency of steady state cavity coupled combustion. To support the combustion

efficiency calculation, many intermediate parameters are useful such as stream thrust, peak pressure ratio, and combustor exit pressure ratio. From these primary objectives, the desire is to understand the phenomena causing the changes so the design can evolve, capitalizing on the advantages of aeroramp injection and mitigating the disadvantages. Improvements in combustion efficiency of as little as 5% will likely make the additional complexity of four times as many injection holes worthwhile in a system design.

## I.4 Research Focus

The research focus is to collect and analyze combustion data with the aeroramp injector hardware designed by Dr. Lance Jacobsen [7] and a baseline round injector. Both injectors are to be installed in the AFRL Propulsion Directorate Research Cell 18 allowing direct comparison between the configurations to perform an analysis to determine any changes for the aeroramp injector. The information required is: stagnation temperature and pressure, fluid mass flows, wall pressures, thrust stand measurements, and calculated combustion efficiency. The facility personnel process all these parameters to engineering units from the raw voltages. The engineering unit values were then post-processed to filter erroneous data, highlight trends and identify sensitivities. From this, the appropriate way to use the aeroramp injector in the design of a supersonic combustor using a cavity flame holder can be determined.

# II. Theory and Previous Research

## II.1 Dual Mode Scramjet

The governing physics indicate that scramjet propulsion provides the highest specific impulse at Mach numbers between six and eight when using hydrocarbon fuels. The specific impulse ($I_{sp}$) of turbojets, ramjets, scramjets, and rockets as a function of Mach number are in Figure 2 below. The values are primarily theoretical, but it shows the relative performance of the different cycles at the full range of Mach numbers.

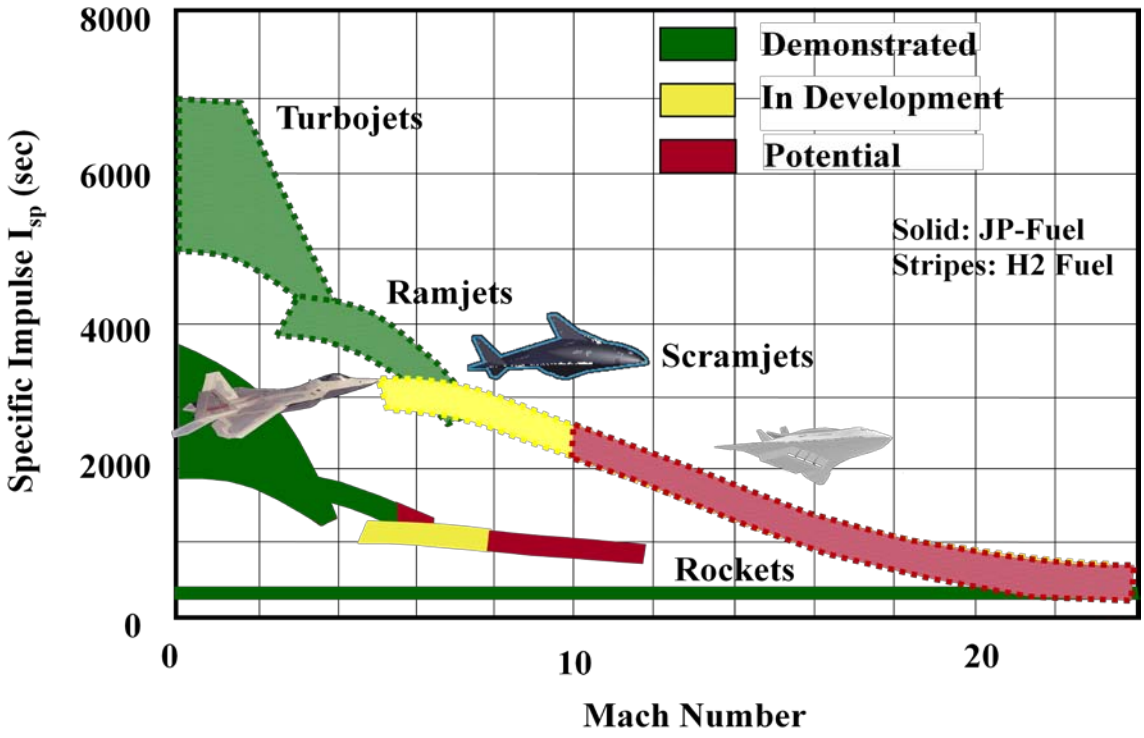


**Figure 2: $I_{sp}$ versus Mach number [8]**

Unfortunately, a significant amount of energy is required to accelerate a vehicle up to operational speeds to take advantage of scramjet propulsion. One method to achieve operational speed is to allow the flow to go subsonic in the combustor and then pass through a thermal throat to exit the combustor supersonically. This dual mode

operation can enable a scramjet flow path to operate at flight Mach numbers as low as 3.5. The primary difference between dual-mode and scramjet mode is the presence of a pre-combustion shock train reducing the average Mach number of the combustor around the flame holder to subsonic speeds. A schematic of a dual mode ramjet, a dual mode scramjet, and a true scramjet can be seen in Figure 3 below.

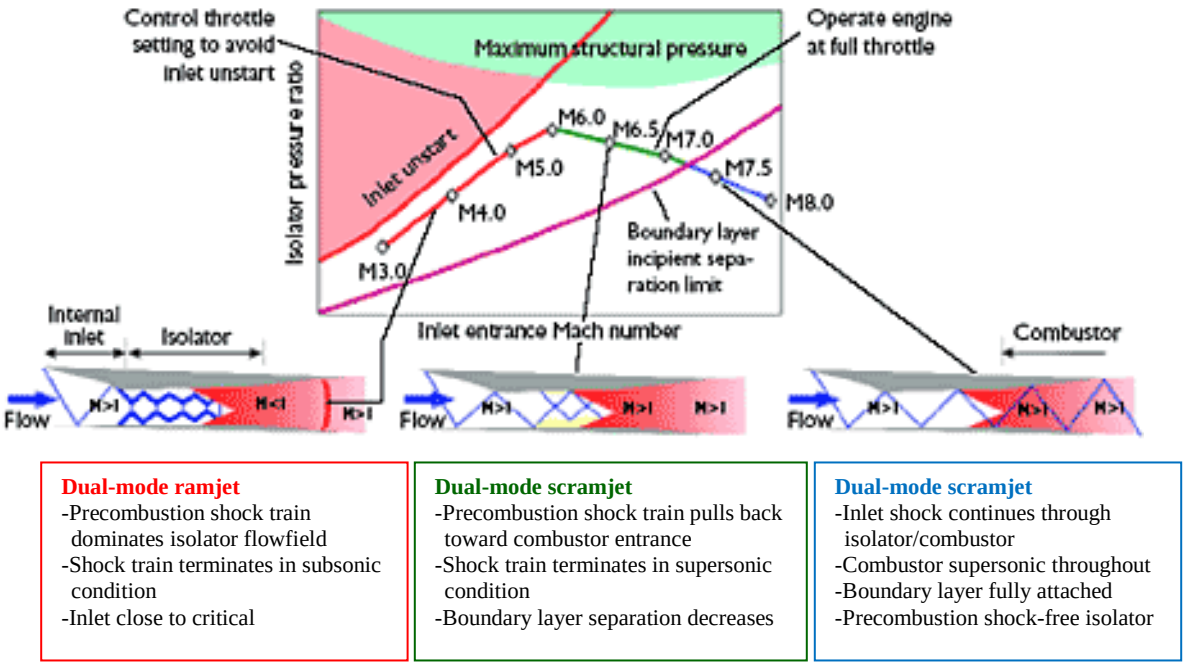


**Figure 3: Modes of operation for a high speed air breathing flow path**

The AFRL Propulsion Research Cell 18 flow path is operated as a dual mode scramjet (DMSJ.) The DMSJ typically cannot operate well below Mach 4.0, but can easily move into full scramjet mode for maximum efficiency cruise or Mach 6.5 or greater acceleration. An alternative is the dual-mode ramjet (DMRJ). The DMRJ is a thermally throated ramjet that typically cannot support full scramjet mode. The DMRJ is typically used when the DMSJ or DMRJ engine takes over as the primary source of thrust between Mach 3.5 and 4.0 is critical, but the need to accelerate beyond Mach 6.0 or

cruise above Mach 5.5 for extended periods is not required. The third mode of operation is scramjet mode. Because of the pre-combustion shock-free isolator, the scramjet mode is the most efficient, but can only be achieved for flight Mach numbers of 6.0 or greater. [9]

## II.2 Motivation for the Aeroramp Injector

The flow through a scramjet combustor has velocities on the order of 6000 ft/s and a minimum average Mach number of approximately 3.0 for a flight Mach number of 6.5. [10] At these speeds, the residence time of the fuel in the combustor is only a few milliseconds making the mixing and combustion of the fuel very challenging. The nominal approach to fuel injection uses a circular injector with a sonic exit angled 15 to 30 degrees above the wall. This design minimizes the total pressure loss from injection while still maintaining adequate mixing and penetration. [11] Both experiments and computational analysis have shown that a way to increase the mixing is to introduce significant vorticity into the flow in the region of the fuel injector. [5]

There are several ways to generate the additional vorticity needed to enhance the mixing of fuel in a supersonic combustor. One practical method is to introduce a highly swept wide physical ramp as shown in Figure 4. The ramp causes compressed air from the top to roll off the sides and circulate into the base area. [5]

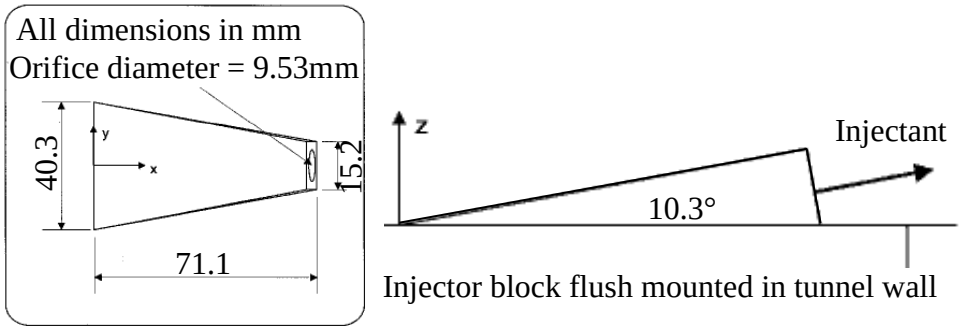


**Figure 4: Physical ramp top and side view [5]**

The resulting vorticity significantly enhances mixing efficiency, but due to the intrusive nature of the ramps and the reduction in flow path area, the total pressure losses for the ramp alone are about 40%. These losses can be mitigated with an expanding wall but only slightly. [5]

Another intrusive design is to put a very narrow strut into the flow, injecting the fuel from locations much closer to the center of the flow path. [12] This design is being analyzed extensively [12] for application in circular flow paths, especially for designs with larger cross sections where the wall injectors cannot penetrate to the center without leaving the walls lean. Preliminary CFD and testing indicate for the same relative mixing, the total pressure losses from the strut are less than for the ramp. [9] This arrangement can be seen in Figure 5 below.

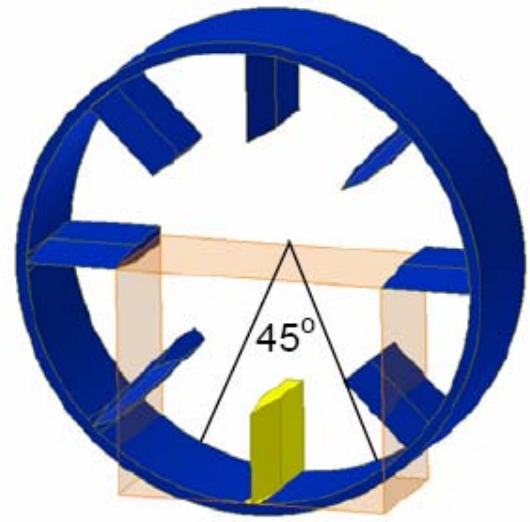


**Figure 5: Strut injector in notional round scramjet Flow path [12]**

The primary weakness of both intrusive fuel injector styles is the cooling required to maintain a pristine shape for aerodynamic vorticity and fuel mixing purposes in a flow with a total temperature exceeding 2000 R.

Yet another method to achieve enhanced mixing is to use the interaction of the jets from the injectors to create the vorticity needed. Many different jet interactions have been studied at many different cross flow Mach numbers. [4] This technique shows great promise in achieving greater penetration while maintaining satisfactory near-field mixing. [9] One method is to arrange several injectors pointed toward each other to cause jet impingement inducing vorticity. The original concept can be seen in Figure 6.

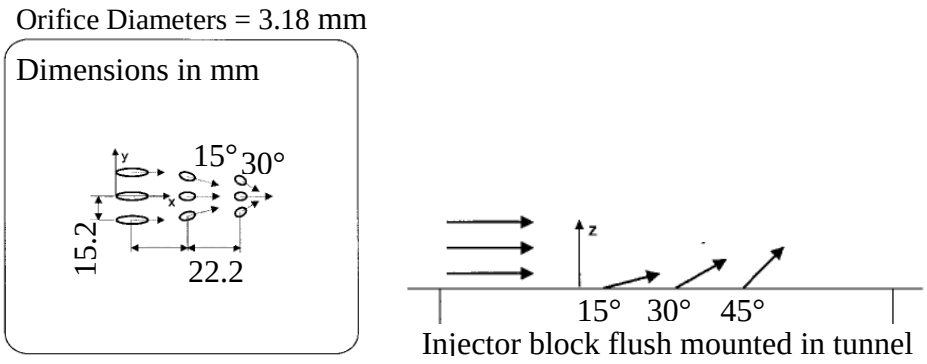


**Figure 6: Aerodynamic ramp top and side view [5]**

This approach is called an Aeroramp injector from the aerodynamic ramp effect created by the interacting plumes from the injector array. The basic design has multiple rows and columns of injectors arranged in close proximity and angled toward each other. The intended result is an interaction of the jets creating better mixing than a single injector without the significant total pressure losses from intrusive mixing devices. Both experimental and computational efforts have shown the aeroramp injectors do have significantly higher vorticity relative to a round injector, similar to that generated by a physical ramp, but without the large total pressure losses. [5]

### II.3 Evolution of the Aeroramp Injector Design

The original design of the aeroramp injector [5] seen in Figure 6 consisted of a nine-hole array composed of three rows of three injectors. The first row of injectors was aligned with the flow and had a fairly shallow angle. The injectors in subsequent rows were progressively angled more toward each other and had steeper angles to the wall to force the fuel away from the wall and into a swirling pattern. This design was tested using helium injected into air to simulate a hydrogen fuel and the results showed the aeroramp injector had slightly lower mixing than the ramps with a much lower total

pressure loss. [5] The complexity of manufacturing the nine-hole array has restricted the practical employment and limited the performance of the aeroramp in comparative tests.

A four-hole aeroramp seen in Figure 7 below was designed to mitigate the extreme complexity of the original aeroramp injector while still preserving the desired counter - rotating vortices. [7]

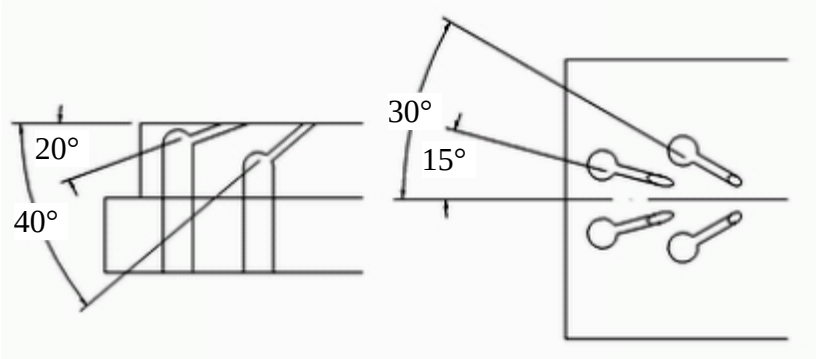


**Figure 7: Improved aeroramp injector angles [13]**

This injector had a greater toe-in angle on the rear jets and eliminated the middle row and center column entirely. The increased toe-in angle on the aft jets increases the mixing and reduces the secondary core left in the shear layer, which could lead to high heating on the wall and, when coupled with a cavity flame holder, could cause a rich blowout. The four-hole aeroramp was design to maximize axial jet-induced vorticity and to use this to lift the entire plume into the flow.

### II.4 Previous Results of Improved Aeroramp Testing

Early tests on the four-hole injector compared the performance of a single array of the improved aeroramp injectors to a single 15-degree round injector. [7] The results showed the aeroramp mixed significantly better than the single hole with about 10% higher total pressure losses. For a supersonic cross flow, the aeroramp also had a plume

encompassing 42% more area as seen in Figure 8 below. The plume is defined as the area encompassed by a line at an $\alpha_{mix}$ of 0.068, the stoichiometric fuel-air ratio of ethylene.

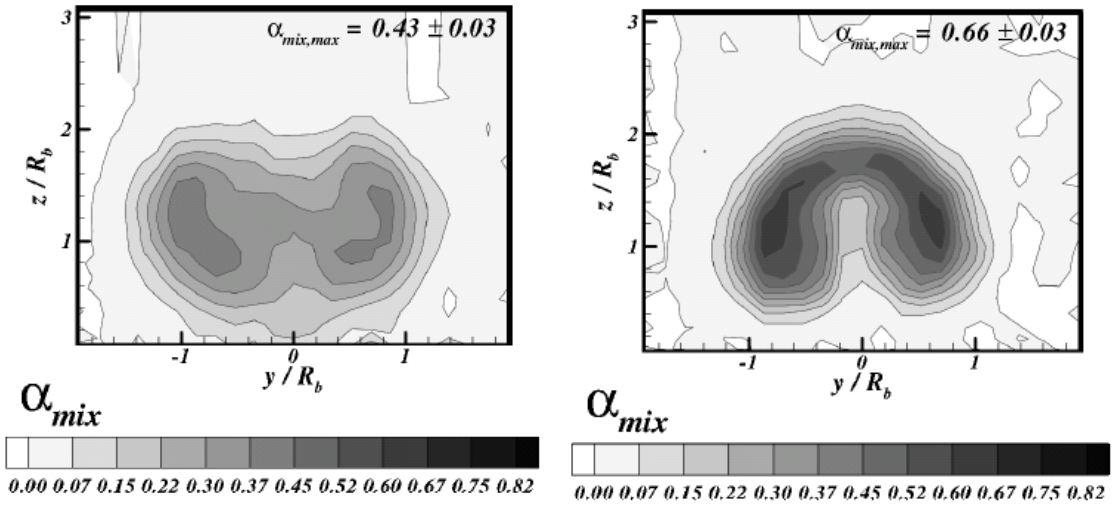


**Figure 8: Fuel concentration for aeroramp (left) and round injector (right) [7]**

The improvement in plume area did not come without a cost, though. While the initial penetration from the aeroramp was higher, it was quickly overtaken by the round injector performance. The aeroramp resulted in a plume larger in area, but closer to the wall than the round injector test case.

When the aeroramp was tested in a cavity-coupled combustor with simulated combustion backpressure, similar trends were noticed. [3] Planar Laser Induced Fluorescence (PLIF) measurements using nitric oxide seeded into the flow field indicated the plume of the aeroramp dissipated more suggesting better mixing over a larger area than the round injector for a Mach 2.0 air flow as seen in Figure 9.

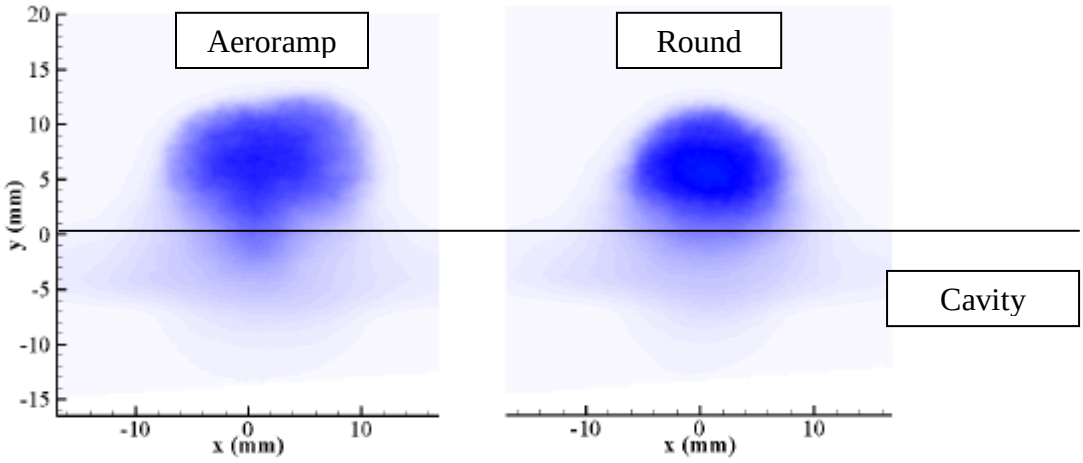


**Figure 9: PLIF average images of aeroramp vs. round injector plumes [14]**

The results also showed the cavity entrainment from the aeroramp injector was significantly higher than the results of the round jet giving a more fuel rich cavity. Because the injected fuel was inert, a correlation to the combustion limits is difficult but these results do give an idea of expected trends.

Further testing on the improved aeroramp configuration focused on the coupling between the aeroramp injector and a plasma torch igniter for engine cold start research. The addition of the plasma torch, especially when coupled closely behind the aeroramp, has a significant effect on the shape of the plume from the aeroramp. The plume stem seen in Figure 9 extends along the lower wall or into the cavity still, but is not as dramatic because the effluent from the torch forces the stem away from the lower wall.

# III. Test Setup and Apparatus

## III.1 Facility Configuration

The experiment occurred on the thrust stand inside Research Cell 18 at Wright-Patterson Air Force Base. This facility was designed for fundamental studies of supersonic reacting flows using a continuous-run, direct-connect, open-loop airflow supported by the Research Air Facility. The test rig consists of a natural-gas-fueled vitiator to heat incoming air beyond what the air facility is capable of, interchangeable facility nozzles (Mach 1.8 and 2.2 currently available), modular isolator, modular combustor, truncated nozzle, and exhaust, as illustrated in Figure 10 below.

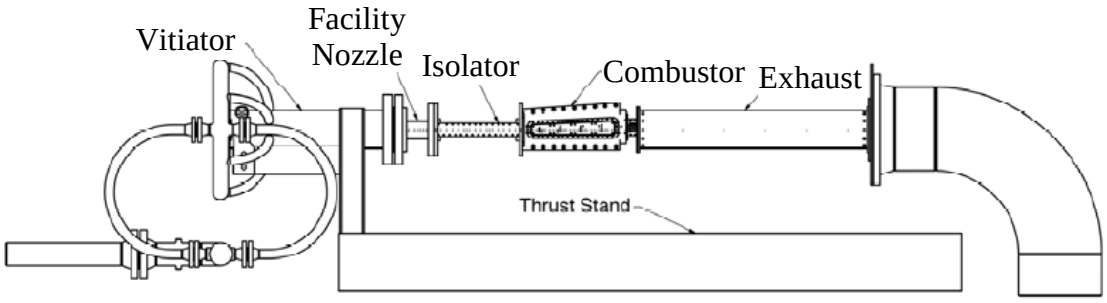


**Figure 10: Air Force Research Lab Propulsion Directorate research cell 18**

The rig is mounted to a thrust stand capable of measuring thrust up to 9.0 kN (~2000 lbf). The facility air supply is capable of providing up to 13.6 kg/s (30 lb/s) of air, with total pressures and temperatures up to 51 atm (750 psia) and 900 K (~1600 R), respectively. An exhaust system with a pressure of 0.24 atm (3.5 psia) lowers and maintains the backpressure for smooth starting and safe operation. Combined with currently available Mach 1.8 and 2.2 facility nozzles, the air vitiator was fine-tuned to simulate discrete flight conditions from Mach 3.5 to 5.0 at flight dynamic pressures up to 96 kPa (2000 psf). The relatively low simulated flight Mach numbers represent the

scramjet takeover conditions, at which dual-mode combustion takes place. The facility Mach numbers equivalencies are derived using nominal inlet efficiencies for the range of operating Mach numbers.

The flow path as tested contains a constant area isolator, a combustor expanding at 2.6 degrees, a 5.0 L/D cavity 5/8 inch deep and a truncated nozzle expanding at 11 degrees. Figure 11 below shows the geometry.

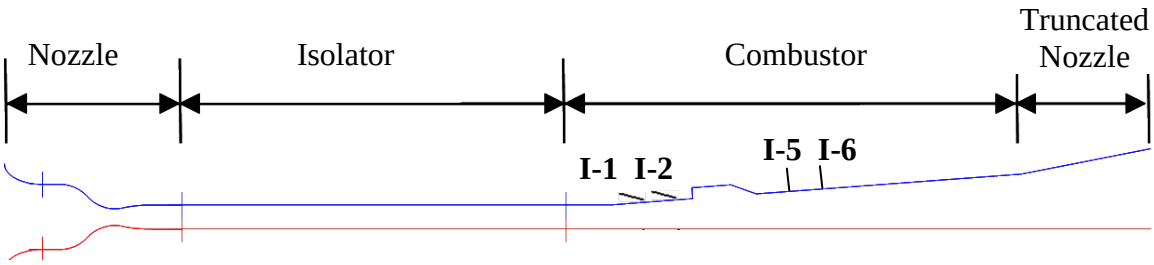


**Figure 11: Research cell 18 scramjet combustor flow path**

The fuel injector locations are annotated as I-1, I-2, I-5, and I-6. I-1 and I-2 are normally round injectors, angled 15-degrees into the flow. I-5 and I-6 are the downstream injectors and are angled normal to the wall. The I-notation simply indicates that it is an injector site rather than an igniter or instrumentation location.

Figure 12 is a photograph of the rig from the isolator through the truncated nozzle and into the facility exhauster.

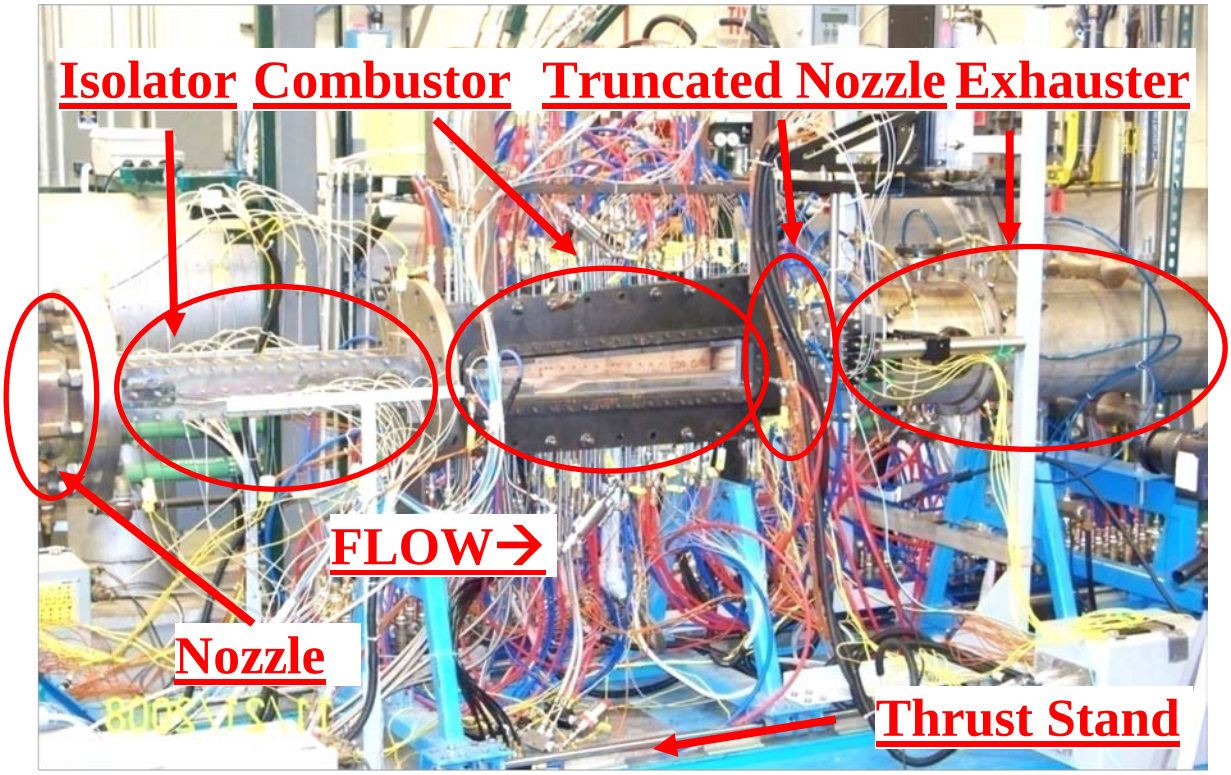


**Figure 12: Research cell 18 scramjet combustor**

The blue frame at the bottom is the thrust stand. Blue and red hoses are used for the water-cooling for the combustor and truncated nozzle. The static pressure tubes can be seen at the left on the isolator.

The aeroramp injector block consisted of two rows of injector arrays corresponding replacing the I-1 at 30.2 and I-2 at 32.2 fueling locations. The I-1 station was not used. Previous testing has shown no performance improvement but a significant reduction in operability for I-1 compared to I-2. A photograph of the injector block in the combustor can be seen at the top of Figure 13.


**Figure 13: Aeroramp injector block installed in rc-18 combustor flow path**

The aeroramp injectors are arrays of four small holes on the top wall. The large circles between the rows of aeroramp injectors are blanks where plasma torches can be installed. The bottom wall shows the baseline injector design that can be either three or four injectors across the width of the flow path. The white coating is a thermal barrier coating used to dissipate shock interactions and extend the life of the hardware.

### III.2 Test Series and Run Procedure

An immense amount of data was collected during this test series so every attempt was made to ensure the run procedure maximized the accuracy and usefulness of the data. The test series encompassed 55 days with 11 run nights and had three major hardware changes. On average, one test was performed each week. Due to the power requirements of the air facility, testing started at about 1800 and ended around midnight. Prior to test

start, significant test preparation occurred to include synchronizing all the data systems and performing basic data system health checks.

Once the air facility was online and the test article reached a thermal equilibrium, the test runs began. Each run had three main phases: vitiator ignition and stabilization, ignition and combustion stabilization, and steady state combustion. The vitiator ignition and stabilization took on the order of two minutes. After the test condition was reached, the combustor fuel isolator valve was opened. If the fuel did not ignite, the two spark plugs in the cavity were started. If combustion was still not initiated, compressed air was injected downstream of the cavity to generate a pre-combustion shock train, raising the pressure and temperature in the combustor in a process known as aerothrottle. The flow rate of the aerothrottle was increased until either combustion was achieved or the pre-combustion shock moved into the facility nozzle creating non-uniform flow. At this point the aerothrottle was turned off.

When the combustor lit, there was a transient phase after the aerothrottle turned off after which point the static pressures stabilized. Once stable, a traverse with a tunable diode laser optic passed the length of the window in the truncated nozzle. The full traverse took about 12 seconds, after which the fuel to the combustor was turned off. Once the combustor had cooled sufficiently, the vitiator was turned off to allow for the heat sink hardware to continue cooling. The cool-down cycle between runs lasted between two and ten minutes depending on how much the temperature had increased during the run. During this time, any adjustments to the test matrix as a result of the previous run were applied and then the process was repeated.

### III.3 Instrumentation Description

The test article used for this experimental series had wall static pressures, temperatures, and mass flow meters. The wall static pressures were collected on a analog-to-digital converter with pressure transducers called the PSI system. The PSI system data was collected at 10 Hz. The actual frequency response of the wall static measurements is not high as there are several feet of Tygon® tubing between the test hardware and the pressure transducer.

Mass flow measurements were taken for all of the facility air including the main air to the vitiator and the air used for the aerothrottle starting device. There were also mass flow meters on the vitiator oxygen and natural gas supplies. The ethylene fuel used in the DMSJ combustor was metered through three valves and four flow meters. The mass flow readings were recorded by a data system called the CAMAC system updating the database buffer about every 0.6 seconds. A simplified schematic of the fluid flow in the combustor can be seen in Figure 14.

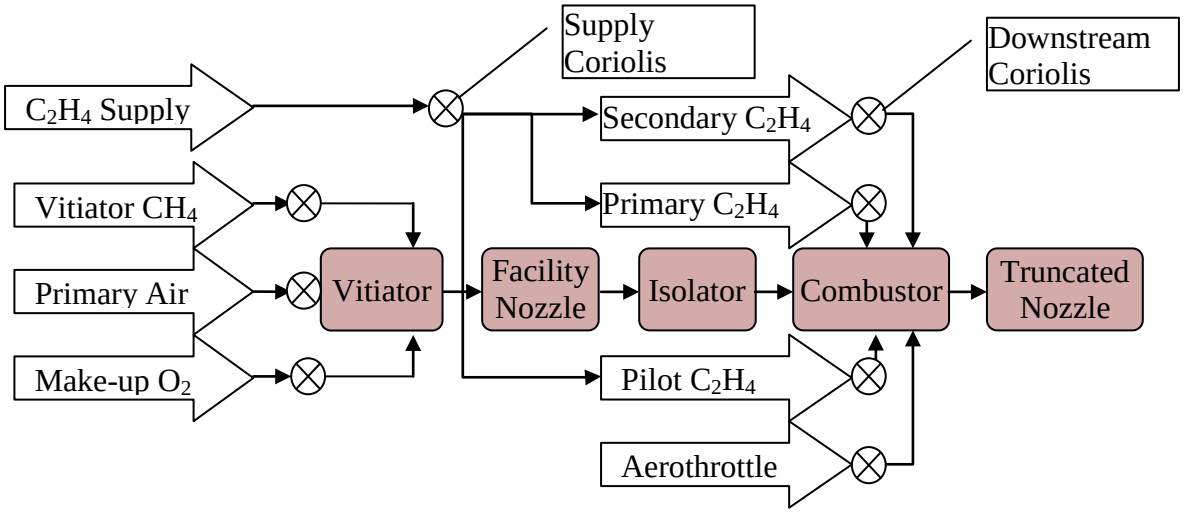


**Figure 14: Schematic of fluid flow in facility**

The ethylene fuel systems consisted of three major systems: the sonic nozzle flow measurements of the Main 1 injector site replaced with the aeroramp injector, the secondary fuel injector site downstream of the flame holding cavity, and the pilot fuel that augments the cavity for fuel-lean conditions. Additionally, there was a Coriolis mass flow meter upstream of the fuel system. This allowed for a verification of the fuel flow rates. During the testing, this instrument was used to identify a problem that forced a replacement in the secondary fuel flow meter.

In early diagnostic testing, the secondary injectors were choking the flow at the injector and thus fouling the sonic nozzle-based flow measurement. For all runs in this experiment including the baseline, the secondary fuel injector mass flow was measured with a separate Coriolis measurement due to the injector block choking concerns. Additionally when the aeroramp was installed, it showed suspicious fuel flow rates. For this reason, the fuel flow rate used for the primary fuel injector was the difference of the upstream Coriolis mass flow meter and the secondary flow rate Coriolis meter.

The ethylene fuel flow rates deviated from nominal desired value. The pneumatic fuel control valves did not have a closed-loop feedback system. The flow rates were manually set which caused some variability in the actual amount of fuel injected. It was determined acceptable because the fuel flow rate remained constant for the duration of any given run and the Coriolis meters gave a measured mass flow with a high degree of accuracy.

Two separate systems collected the thermocouple data and processed it for the data collection system: the CAMAC system was also used for the mass flow meters and a

dedicated thermocouple data system outputting data to the database buffer about every 1.5 seconds. A schematic of the data collection system can be seen in Figure 15.

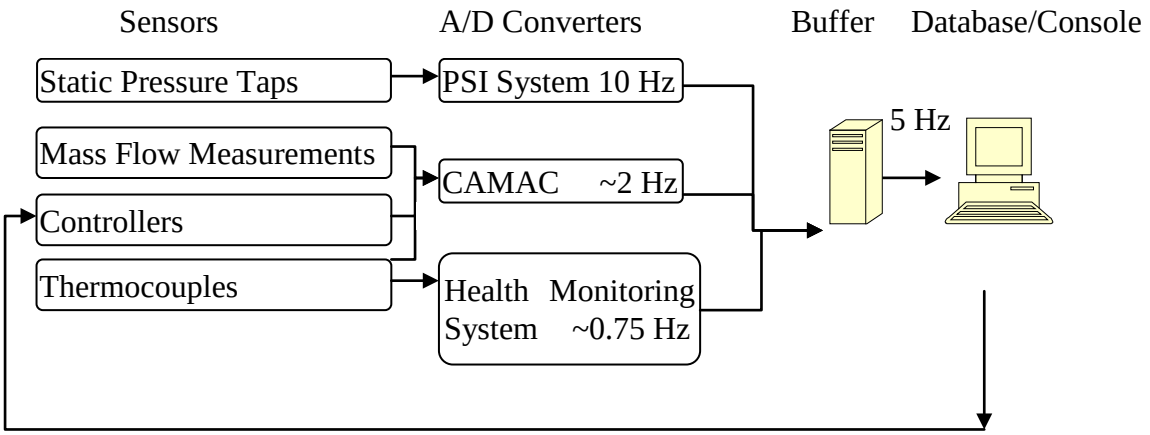


**Figure 15: Simplified schematic of data acquisition system**

The entire flow paths as well as all gas and water supply manifolds were instrumented with type K thermocouples with an accuracy of +/- 2.2R. The thermocouples in the flow path are a mixture of flow surface temperature, temperatures near the flow path surface, temperatures near the back surface of the flow path wall and several on the backside of the flow path wall. The relative depth of the different types of thermocouple installation can be seen in Figure 16.

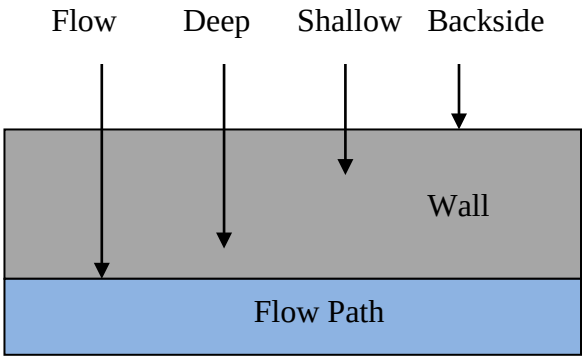


**Figure 16: Nominal thermocouple layout**

### III.4 Test Matrix

Test conditions were selected to match nominal flight conditions for the dual mode operation range assuming a moderate inlet loss. These conditions were chosen based on the facility constraints which were designed to address the challenging dual-mode takeover and acceleration conditions. The nominal conditions for all cases analyzed can be seen in Table 1.

**Table 1: Nominal test conditions**

| Case | Flight M | Flight Q | Primary Φ | Secondary Φ |
|---|---|---|---|---|
| 1 | 5 | 1000 | 0.6 | 0 |
| 2 | 5 | 1000 | 0.9 | 0 |
| 3 | 5 | 1000 | 0.6 | 0.3 |
| 4 | 4.5 | 1000 | 0.6 | 0 |
| 5 | 5 | 1000 | 0.6 | 0.3 |
| 6 | 4.5 | 1000 | 0.6 | 0.3 |
| 7 | 4 | 2000 | 0.3 | 0.3 |
| 8 | 4 | 2000 | 0.3 | 0.3 |
| 9 | 3.5 | 1000 | 0.3 | 0.3 |
| 10 | 3.5 | 1000 | 0.3 | 0.6 |
| 11 | 3.5 | 1000 | 0.3 | 0.3 |
| 12 | 3.5 | 1000 | 0.3 | 0.6 |

The flight Mach number and dynamic pressure Q (in psf) is representative of the expected takeover conditions for a DMSJ based vehicle. Mach 3.5 is at the very low end of where a thermally throated ramjet is theoretically feasible. The total temperature at

Mach 5 is the highest temperature achievable in the facility as it is currently configured. True scramjet mode is not expected until the flight Mach number reaches at least 6.0. Thus, the conditions compared span the entire Mach range of the facility to allow for a comparison of the aeroramp injector throughout the entire dual mode envelope.

Data was collected for these conditions for both the aeroramp and the circular round injector configurations. The secondary site column indicates where the downstream fuel was being injected. I-5-4 is an array of four injectors injecting normal to the flow located at station 40.75 and I-6-4 is also four normal injectors that are located at 42.75.

### III.5 Data Processing and Calculation Methods

To determine the properties for a given run condition while accounting for the cyclic instabilities in the system, four seconds of data was averaged for the combusting condition and two seconds of data was averaged for the non-combusting "tare" of each run. The tare was determined at the time closest to the actual combustion where the facility conditions most matched the run conditions. The heat sink isolator hardware and the water-cooled combustor warmed significantly during the run causing a shift in the isolator shock train position due to boundary layer growth. The movement of the shock train caused a significant change in the overall performance of the combustor so the desired data sampling was taken as close to the end of the run as possible. Four seconds was determined to be enough data to be a representative steady state average because the slowest sensor response, the thermocouples, is roughly 1.5 seconds. Therefore, to capture at least two unique samples, a minimum of three seconds is required. The four

seconds of combusting data was selected from an average of 15 seconds of total combustion time based on the uniformity of the fuel and air inputs and the wall temperatures

All data was recorded from a buffer every 0.2 seconds and used for online data analysis, facility health monitoring, and archived to be used for offline data analysis. The buffer was updated at various intervals depending on the type of instrument collecting and digitizing the data. Because of the data rates and recording time differences, there are many exact duplicate readings in the data set for a given channel from the CAMAC system and the thermocouple system. The data was filtered by discarding up to two identical samples for channels taken with the CAMAC system and up to eight duplicates for the thermocouple system.

The parameters used to calculate performance and operability were the shock train position, the combustion efficiency, the stream thrust, the peak pressure ratio, and the combustor exit pressure. The shock train position was defined as where the first axial static pressure tap showed a ratio from combusting to non-combusting conditions exceeding 1.1. Peak pressure ratio is defined as the maximum static pressure, occurring at the back of the flame holder, divided by the first static pressure in the isolator. Combustor exit pressure was the average of the last two centerline taps in the combustor, one on the body (top) wall and one on the cowl (bottom) wall.

The primary performance measurement was combustion efficiency. Stream thrust includes many of the highly weighted parameters in combustion efficiency. Because of that stream thrust was analyzed independently to provide performance insights. Stream thrust is defined as the thrust produced by the fluid inside the flow path. [15] Figure 17

shows the numbering conventions used in the equations that describe stream thrust and combustion efficiency.

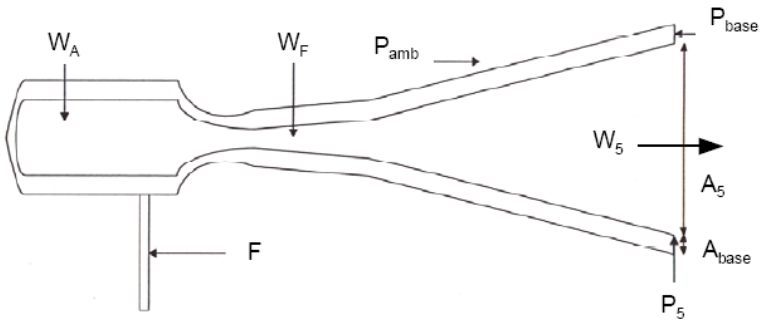


**Figure 17: Schematic for stream thrust and combustion efficiency calculations**

Equation 1 below defines stream thrust as used in this research as simply $ST_5$

Conservation of Momentum:

$$W_5 U_5 + P_5 A_5 = ST_5 = F + P_{amb} A_5 + (P_{amb} - P_{base}) A_{base} \quad (1)$$

The combustion efficiency calculation is performed using the in-house QPERF one-dimensional code simultaneously solving equations 1 through 6 to determine combustion efficiency. As seen, combustion efficiency is based on measurements of the reactant mass flow rates, load-cell forces, heat loss, base pressure, exit pressure, and ambient pressure. Mass fraction of unburned fuel ($Y_{Froz}$) is estimated for and solved iteratively until the density from Equation 2 matches the result from Equation 5. Additional details on the combustion efficiency calculation can be found in Reference (16).

Conservation of Mass: $\rho_5 U_5 A_5 = W_A + W_F = W_5$ (2)

Conservation of Energy: $W_5 \left(H_5 + \frac{1}{2} U_5^2\right) = W_A \left(H_A + \frac{1}{2} U_A^2\right) + W_F (H_F + \frac{1}{2} U_F^2)$ (3)

Momentum solved for Velocity: $U_5 = \left(\frac{ST - PA}{W}\right)_5$ (4)

Mass solved for Density $\rho_5 = \frac{(P_5 * MW)}{R_u * T_5}$ (5)

Combustion Efficiency Definition: $\eta_c = 1 - Y_{Froz}$ (6)

To determine the error of the stream thrust and combustion efficiency calculation, the system precision and bias were calculated with a rigorous build-up from the components through the data acquisition system. The bias and precision were added together to determine the systematic error of the system. The z-distribution based 95% confidence interval standard error of the data points analyzed was then geometrically added to the systematic error. As a sample, the error margins for run F08297AW can be seen in Table 2 below.

**Table 2: Performance parameter uncertainty [16]**

| Parameter | Bias | Precision | Total |
|---|---|---|---|
| Static Pressure | 0.8% | 0.5% | 0.96% |
| Stream Thrust | 1.23% | 0.9% | 1.52% |
| Comb. Efficiency | 4.05% | 3.0% | 5.04% |

As part of the error analysis, a sensitivity study was performed to determine the influence of a 1% change in input to the final combustion efficiency and stream thrust. The results can be seen in Figure 18 below.

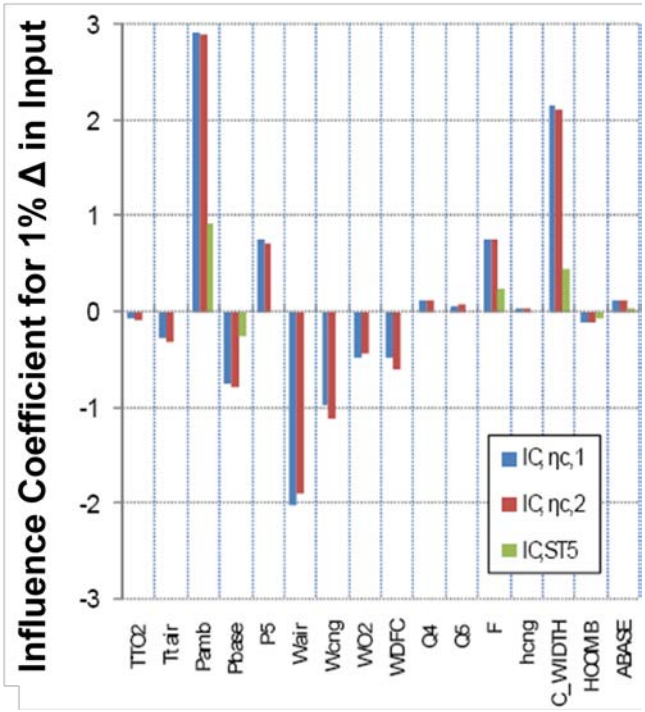


**Figure 18: Combustion efficiency input parameter influence coefficient**

Many of these parameters are fixed or controlled and known very well. For example, the width of the combustor is very unlikely to change when using heavy-weight heat-sink hardware. Likewise, the ambient pressure is very simple to collect with high accuracy. The exit pressure (P5), base pressure (Pbase), thrust stand force (F), and ethylene fuel flow rate (WDFC) are difficult to measure accurately and a very sensitive to the combustion process. These four parameters are captured in the stream thrust as well.

# IV. Results and Discussion

The primary objectives were to determine the operability and performance differences between the aeroramp injector and the baseline 15 degree round injectors. Shock train position is the parameter of primary concern for operability between two runs with the ignition limits being the secondary operability criteria. Performance change is ultimately determined by a difference in the combustion efficiency of the two configurations. To support the combustion efficiency calculation, many intermediate parameters are used such as the stream thrust, the peak pressure ratio, and the combustor exit pressure.

The Mach numbers and dynamic pressures in Table 1 show the intended test conditions, but the translation of those parameters into conditions that can be tested is done before the test. The result is that the vitiator controls to a specified exit temperature and pressure. The actual conditions tested are shown in Table 3 on the following page with a brief summary of the critical data. The case numbers represent pairs of similar conditions corresponding to the intended conditions in Table 1. Run is the unique run identifier from the actual test where the three digit number represents the Julian date of the test for which all facility configurations are constant. The pressure and temperature are the average conditions at the exit of the vitiator. Equivalence ratio ($\Phi$) was calculated by dividing the measured combustor fuel flow rate by the calculated vitiator exit mass flow, and normalizing by the stoichiometric fuel/air ratio for ethylene fuel.

**Table 3: Actual run conditions and summary results**

| Case | Run | $PT_4$ (psi) | $PT_5$ (R) | Prim Φ | Sec Φ | Total Φ | Burned Φ | Stream Thrust(lbf) | $\eta_c$ | Shock Pos(L/H) |
|---|---|---|---|---|---|---|---|---|---|---|
| 1 | 297AW | 102.4 | 1940 | 0.52 | 0.00 | 0.52 | 0.31 | 129 | 0.60 | 19.0 |
| 1 | 303AH | 102.2 | 1952 | 0.53 | 0.00 | 0.53 | 0.35 | 133 | 0.65 | 15.2 |
| 2 | 297AY | 101.8 | 1950 | 0.72 | 0.00 | 0.72 | 0.40 | 176 | 0.55 | 11.9 |
| 2 | 303AJ | 103.6 | 1951 | 0.70 | 0.00 | 0.70 | 0.38 | 159 | 0.54 | 10.8 |
| 3 | 297AX | 102.2 | 1949 | 0.51 | 0.28 | 0.79 | 0.38 | 158 | 0.48 | 19.0 |
| 3 | 303AM | 102.2 | 1950 | 0.48 | 0.26 | 0.75 | 0.34 | 139 | 0.46 | 15.2 |
| 4 | 297AK | 102.5 | 1790 | 0.52 | 0.00 | 0.52 | 0.32 | 142 | 0.62 | 19.0 |
| 4 | 303AP | 103.0 | 1791 | 0.60 | 0.00 | 0.60 | 0.40 | 160 | 0.66 | 10.8 |
| 5 | 297BA | 101.6 | 1950 | 0.50 | 0.28 | 0.78 | 0.36 | 152 | 0.46 | 19.0 |
| 5 | 303AU | 102.6 | 1950 | 0.52 | 0.26 | 0.78 | 0.38 | 146 | 0.48 | 14.1 |
| 6 | 297AL | 103.4 | 1794 | 0.51 | 0.28 | 0.79 | 0.36 | 158 | 0.45 | 15.2 |
| 6 | 303AV | 103.0 | 1793 | 0.53 | 0.27 | 0.80 | 0.35 | 152 | 0.44 | 10.8 |
| 7 | 301AL | 101.1 | 1390 | 0.32 | 0.29 | 0.60 | 0.23 | 182 | 0.38 | 9.7 |
| 7 | 308AH | 101.8 | 1389 | 0.29 | 0.27 | 0.56 | 0.21 | 183 | 0.38 | 7.5 |
| 8 | 301AN | 101.2 | 1389 | 0.30 | 0.28 | 0.58 | 0.23 | 191 | 0.39 | 9.7 |
| 8 | 308AK | 102.7 | 1391 | 0.27 | 0.27 | 0.55 | 0.22 | 191 | 0.40 | 6.4 |
| 9 | 301AO | 51.5 | 1254 | 0.31 | 0.29 | 0.60 | 0.24 | 107 | 0.40 | 9.7 |
| 9 | 308AP | 52.3 | 1254 | 0.30 | 0.30 | 0.61 | 0.26 | 110 | 0.42 | 4.2 |
| 10 | 301AP | 51.9 | 1252 | 0.30 | 0.51 | 0.81 | 0.25 | 112 | 0.31 | 8.6 |
| 10 | 308AS | 52.4 | 1255 | 0.30 | 0.50 | 0.80 | 0.26 | 113 | 0.33 | 3.0 |
| 11 | 301AC | 51.4 | 1250 | 0.32 | 0.30 | 0.62 | 0.23 | 100 | 0.37 | 10.8 |
| 11 | 308AX | 52.3 | 1255 | 0.30 | 0.29 | 0.59 | 0.22 | 101 | 0.37 | 7.5 |
| 12 | 301AD | 52.4 | 1255 | 0.29 | 0.50 | 0.79 | 0.23 | 111 | 0.29 | 9.7 |
| 12 | 308AY | 52.2 | 1253 | 0.29 | 0.57 | 0.86 | 0.24 | 106 | 0.28 | 5.3 |

## IV.1 Operability

There were two main metrics of operability used to compare the aeroramp injector to the baseline injector: the conditions where combustion was sustained and the location of the shock train for a given combusting configuration.

### *IV.1.1 Combustion Limits*

The range of operable conditions for the aeroramp injector was significantly less than for the baseline injectors. The combustor could be ignited with the baseline injectors and an aerothrottle for virtually all conditions tested from Mach 3.5 to 5 and free stream

equivalent dynamic pressures of 500 psf to 2000 psf. When the aeroramp was installed, it was not possible to sustain combustion at 500 psf dynamic pressure once the aerothrottle was turned off. To sustain combustion at 2000 psf with the aeroramp it was required to light the cavity pilot first using only pilot fuel and then add the main fuel once the pilot was stabilized while the pilot was still being fueled. Once the main fuel was lit and stabilized, the pilot fuel was removed. The 2000 psf cases were the only cases analyzed that used any pilot fueling.

For all conditions where the aeroramp did not work, whether at 500 or 2000 psf equivalent dynamic pressure, the local equivalence ratio in the cavity was too high to sustain combustion. This assertion is based on the inability to achieve ignition despite the direct fueling of the cavity. Ignition with direct fueling of the cavity with no main fuel can be achieved at an equivalence ratio of about 0.01. Figure 9 shows in a Mach 2.0 flow, the aeroramp plume with its higher vorticity has a stem drawn through the cavity shear layer. A similar phenomena would occur in locally subsonic flow caused by the pre-combustion shock because there is still a fuel-rich region against the cavity shear layer. The resulting high concentration of fuel in the recirculating cavity could cause a rich blowout. Additionally the soot buildup on the base of the cavity seen in Figure 24 confirms that the cavity was very fuel rich.

A second possibility for the decreased operability range is the jet momentum of the aeroramp injector at low and high flow rates does not perform as designed. At low flow rates jet interaction may be less than desired such that penetration is adversely affected. The resulting fuel rich boundary layer would be entrained in the cavity and cause combustion to be unsustainable. Additionally if the jet momentum is too high, it could

cause the plumes from the four arrays to interact and create an aerodynamic ramp the width of the combustor rather than four independent aerodynamic ramps. This large ramp could force compression of the air above the cavity preventing any significant quantities of air from entering the cavity. This would also create a perceived fuel rich cavity scenario. The current data set that has been analyzed does not have sufficient information to conclusively determine what is happening.

### *IV.1.2 Isolator Margin*

While the inability to maintain or initiate combustion over a broad range of fueling conditions is a significant issue, an equally important measure of operability is the ability of the combustor to not force the pre-combustion shock train out of the isolator and, in a full engine with inlet, cause an inlet unstart and likely catastrophic loss of thrust. This property is most commonly expressed in diameters or duct heights of isolator remaining in front of the pre-combustion shock. The location of the pre-combustion shock is primarily driven by the pressure in the combustor which in turn is driven by the amount of heat being released through combustion. The comparison of shock position relative to total $\Phi$ can be seen in Figure 19.

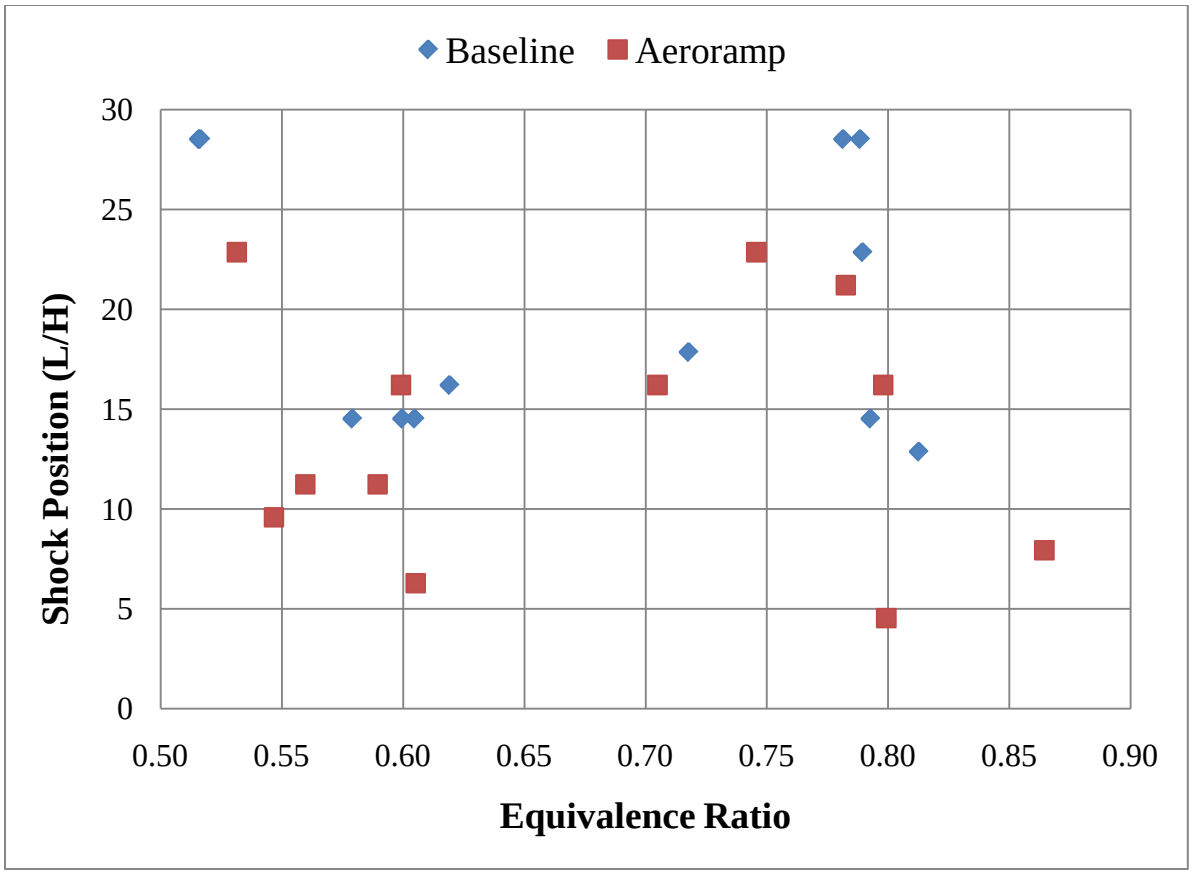


**Figure 19: Shock position versus total equivalence ratio**

When the shock position reaches 1.5 or below, the combustor is considered unstarted. Any unstart cases are not included in further analysis. It is obvious that there is no clear correlation for the shock position versus the equivalence ratio in either the baseline or the aeroramp. There does appear to be a weak trend that the aeroramp has less isolator margin than similar baseline configurations, though. One reason the trend may not be strong is that some of the fuel is being injected downstream of the flame holder.

The purpose of the downstream injection is to increase the thrust at low Mach numbers while preserving a started isolator and inlet. Increasing the thrust is accomplished by injecting the fuel downstream of the flame holder in a section of the combustor with larger relative area. The intention is the scramjet will take over from a

booster at a slower condition. [10] In order to explore this effect, the shock train position relative to only the primary fuel injection equivalence ratio was examined in Figure 20 below.

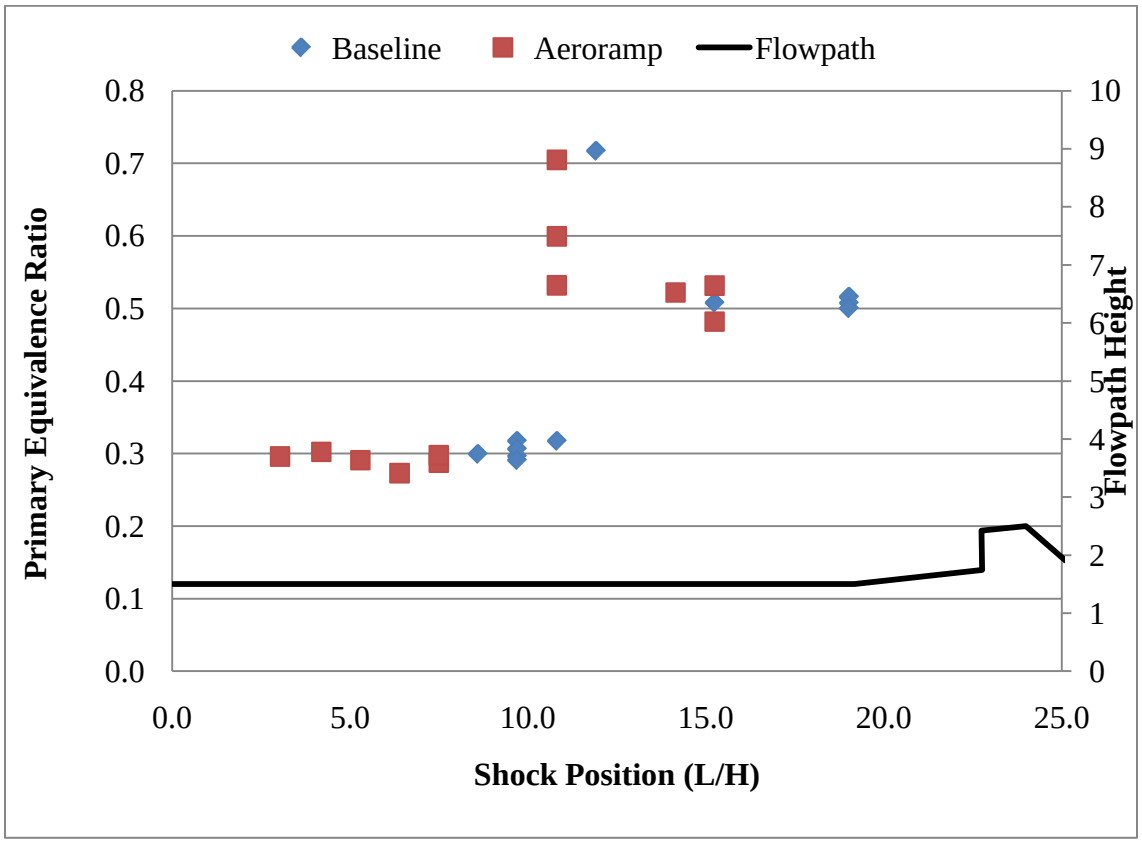


**Figure 20: Shock train position versus primary equivalence ratio**

Of note in Figure 20, the data is grouped into two sets, with the ones around a Φ of 0.3 corresponding to the Mach 1.8 facility nozzle and the higher fueling conditions correlating to the Mach 2.2 facility nozzle. For both sets, when compared to only the primary equivalence ratio, there is a very strong relationship between the baseline and the aeroramp configurations. The aeroramp has consistently less isolator margin, even to the point where the best aeroramp cases are matched with the worst baseline cases. To determine the cause of this strong negative impact, a static pressure trace is presented in

Figure 21 below for Case 1. From Figure 21 the reduced isolator margin is certainly related to a higher pressure rise in the combustor relative to the baseline configuration.

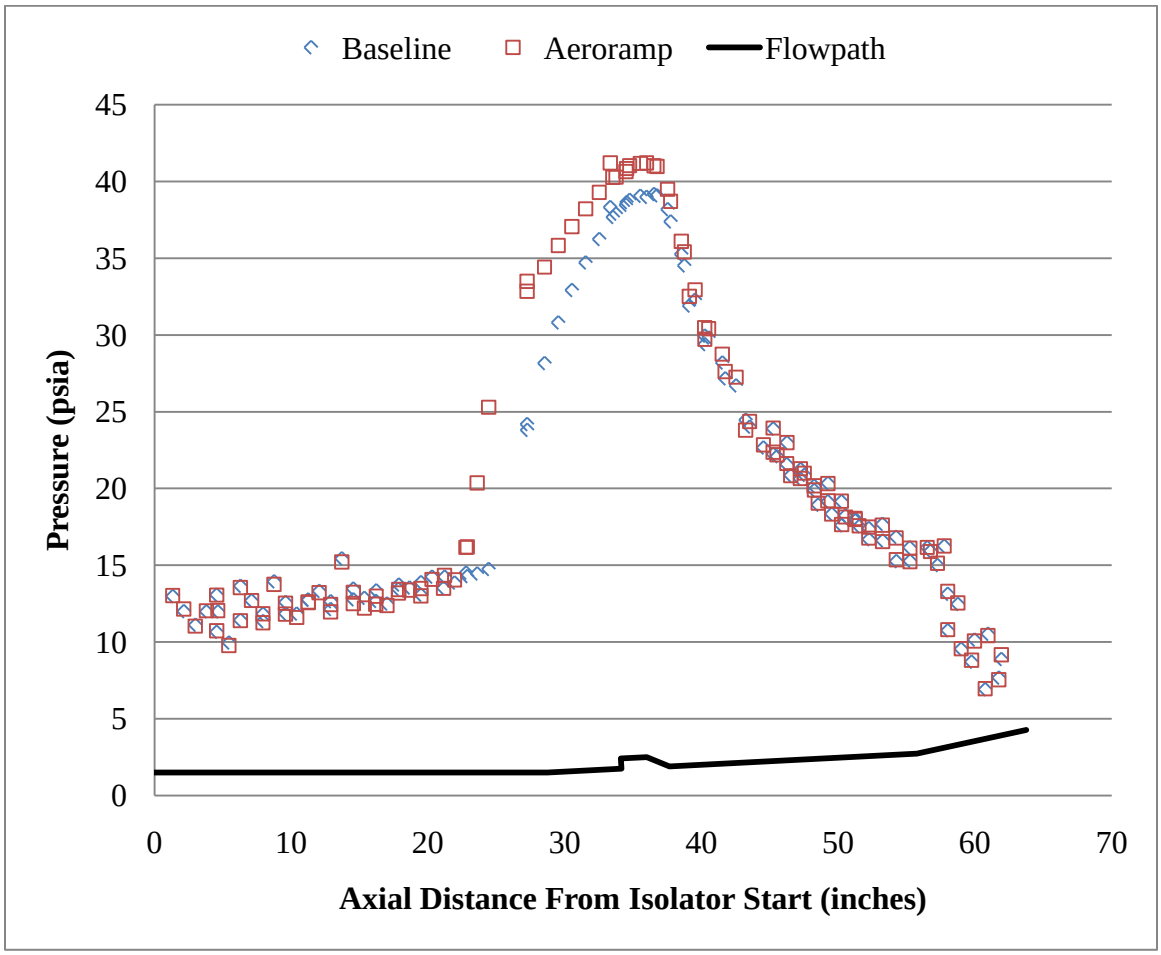


**Figure 21: Axial wall static pressure (case 1- mach=5, q=1000, φ=0.52/0.0)**

### *IV.1.3 Peak Pressure Ratio*

There is a very strong correlation between the peak pressure in the combustor and the isolator shock position. [17] To determine the cause of the reduced isolator margin, the peak static pressure normalized by the isolator

entrance static pressure was compared for similar cases as seen in Figure 22 below.

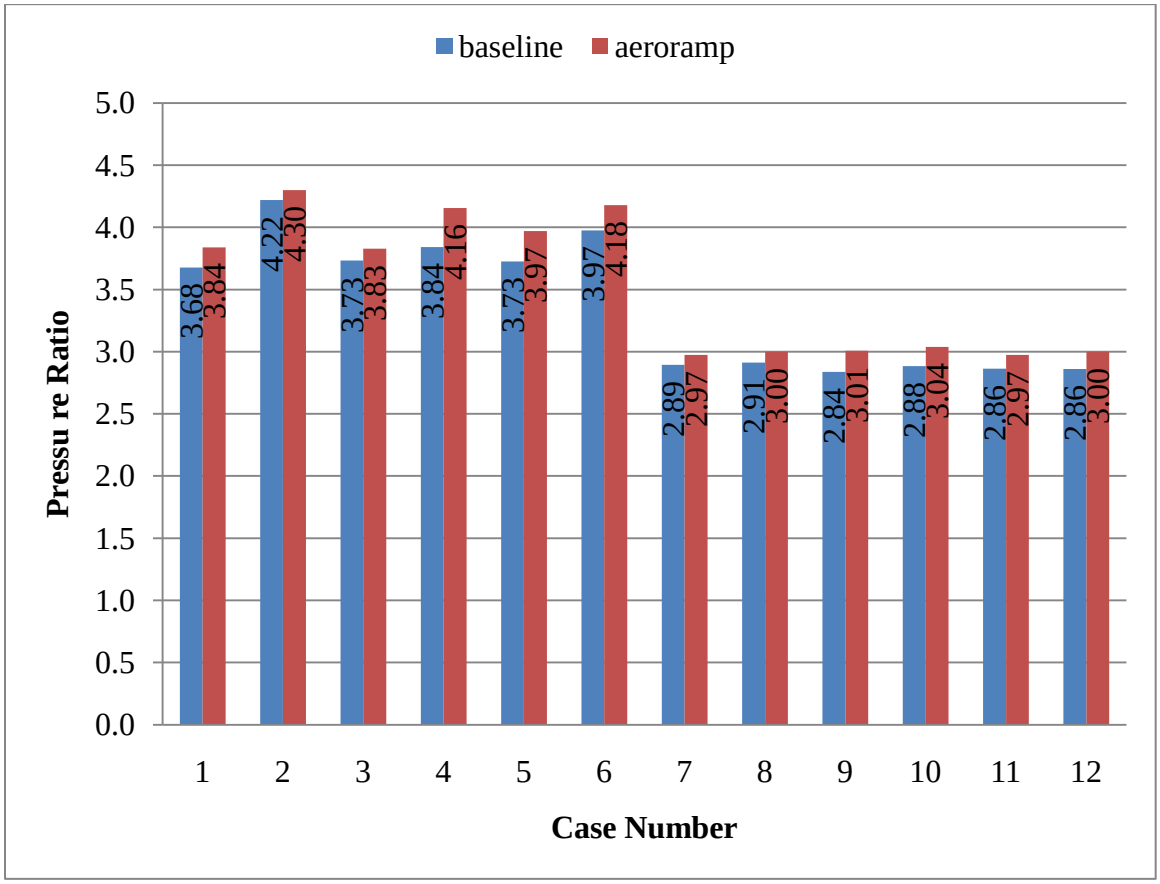


**Figure 22: Peak pressure ratio comparison by case**

The peak pressure is consistently higher for the aeroramp injector. The higher peak pressure ratio is typically the result of additional combustion such as the change from Case 1 to Case 2 where the primary fuel flow is 50% greater. The absence of that variation in Cases 7-12 where the Mach 1.8 nozzle is used indicates that the combustion process is fuel saturated and that as additional fuel is added, no additional enthalpy increase as result of combustion and corresponding pressure rise is occurring.

A plot of the burned equivalence ratio defined as the combustion efficiency multiplied by the total equivalence ratio is seen in Figure 23.

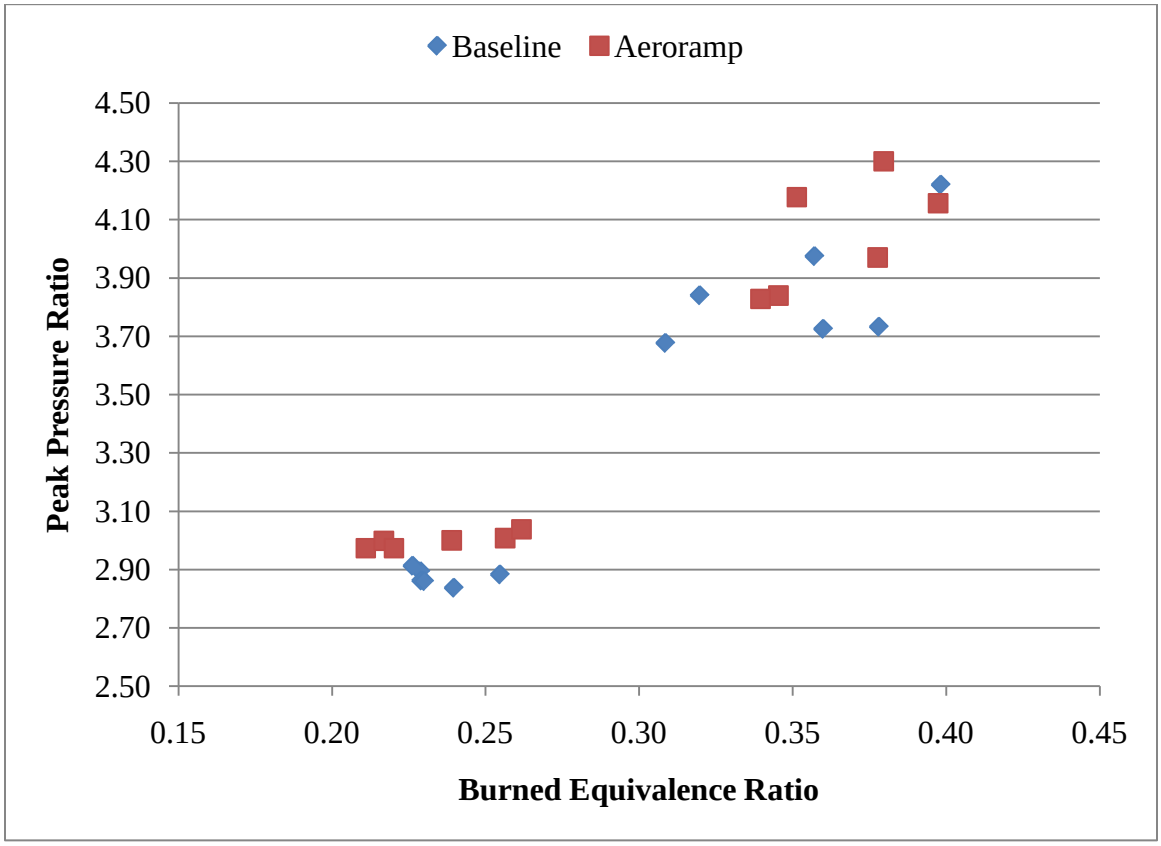


**Figure 23: Peak pressure ratio compared to burned equivalence ratio**

The peak pressures are definitely responding to the actual amount of fuel that is being burned. There is a distinct increase for the aeroramp injector at the Mach 1.8 nozzle grouping on the lower left that is causing the operability reduction at low Mach numbers. The Mach 2.2 nozzle group does not seem to have a systematic difference. The aeroramp is generally higher, but the difference is not as pronounced as for the Mach 1.8 nozzle.

Further verification that the aeroramp injector in particular is creating a fuel-rich cavity can be seen in the following photographs of the flow path after F08308, the day the Mach 1.8 nozzle was installed.


**Figure 24: Soot in the cavity after F08308 runs**

The heavy sooting shows excessive amounts of fuel were being dumped into the cavity. The following run burned the soot off the wall in just a few seconds so this is not a cumulative build up over many days, but rather the result of one or a few previous runs. The most buildup is in the area around the spark plugs so it is not hard to imagine that the local equivalence ratio could be too high for combustion in similar cases.

## IV.2 Performance

The distribution of static pressure seen in the previous section is a preliminary indicator that while the operability is different, the performance of the combustor with the two different injectors may not be significantly different. This is because in the aft portion of the combustor, where the axially oriented area is the greatest, the pressures are very similar.

### *IV.2.1 Combustion Efficiency ($\eta_C$)*

The most obvious but complicated performance metric to analyze is the combustion efficiency. Figure 25 below shows the comparison of the combustion efficiency as a function of the total equivalence ratio for both injector configurations.

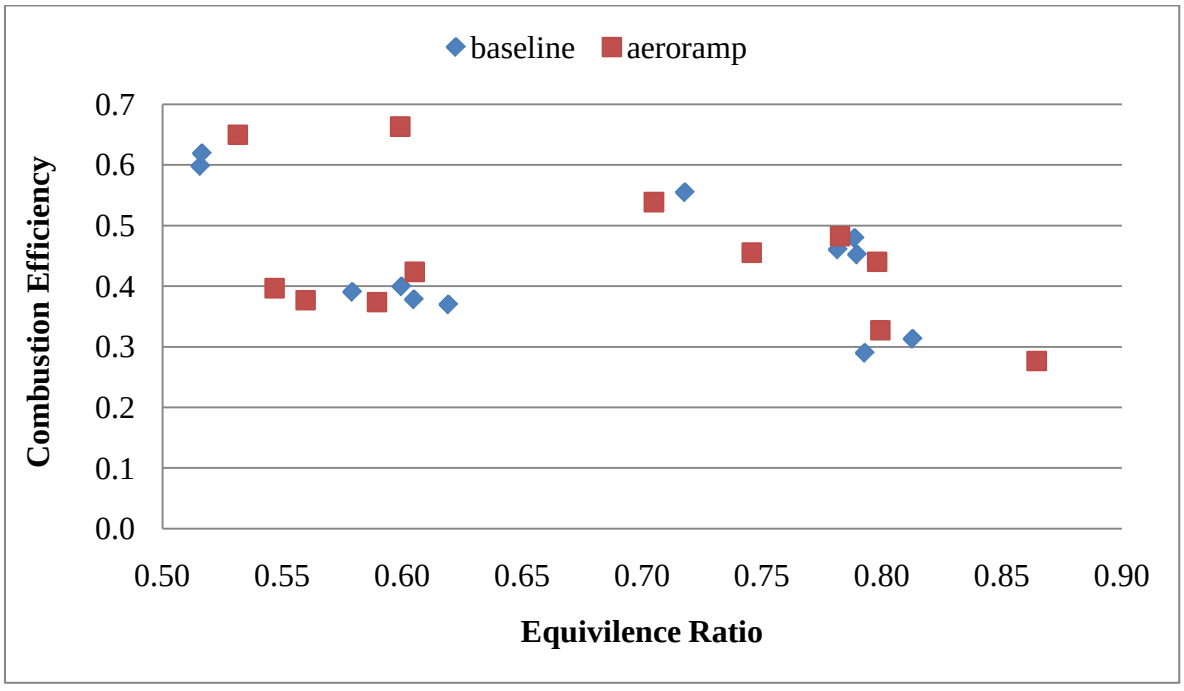


**Figure 25: Combustion efficiency versus total equivalence ratio**

Scramjet combustion efficiencies are typically in the range of 50-80% with at least 70% desired. The extremely low efficiencies seen in the higher equivalence ratios in Figure 25 make the accuracy of the inputs to the QPERF combustion efficiency calculation suspect. The online QPERF running during the test that was used to calculate the values seen in Figure 25 was compared against an offline calculation to verify the accuracy of the efficiency calculation. When the offline efficiency calculation was performed, estimates that are more accurate were made of several parameters including exit pressure and base pressure. The online efficiency uses only one of the two static pressure taps near the exit of the combust so for the offline comparison an average of the last station taps was used. Another area that the assumptions were improved is the base force calculation. The online calculation uses the true average of 12 base pressure taps, but the actual area of the base is highly weighted toward six of those taps. For the offline case, it was assumed that those six taps were representative of 70% of the force on the base. The final result was less than 2% different from the online calculation so it was concluded that the exit and base pressures were not the primary source of error. Another parameter that may be causing the differences is the heat flux. The current facility does not have a heat flux measurement so it has been assumed to be zero. The addition of that measurement will likely increase the accuracy of the 1-D calculations.

To determine any possible correlations between the data appearing in the expected 60-80% range, the same information was plotted by test case in Figure 26. The red squares are the aeroramp run for each condition.

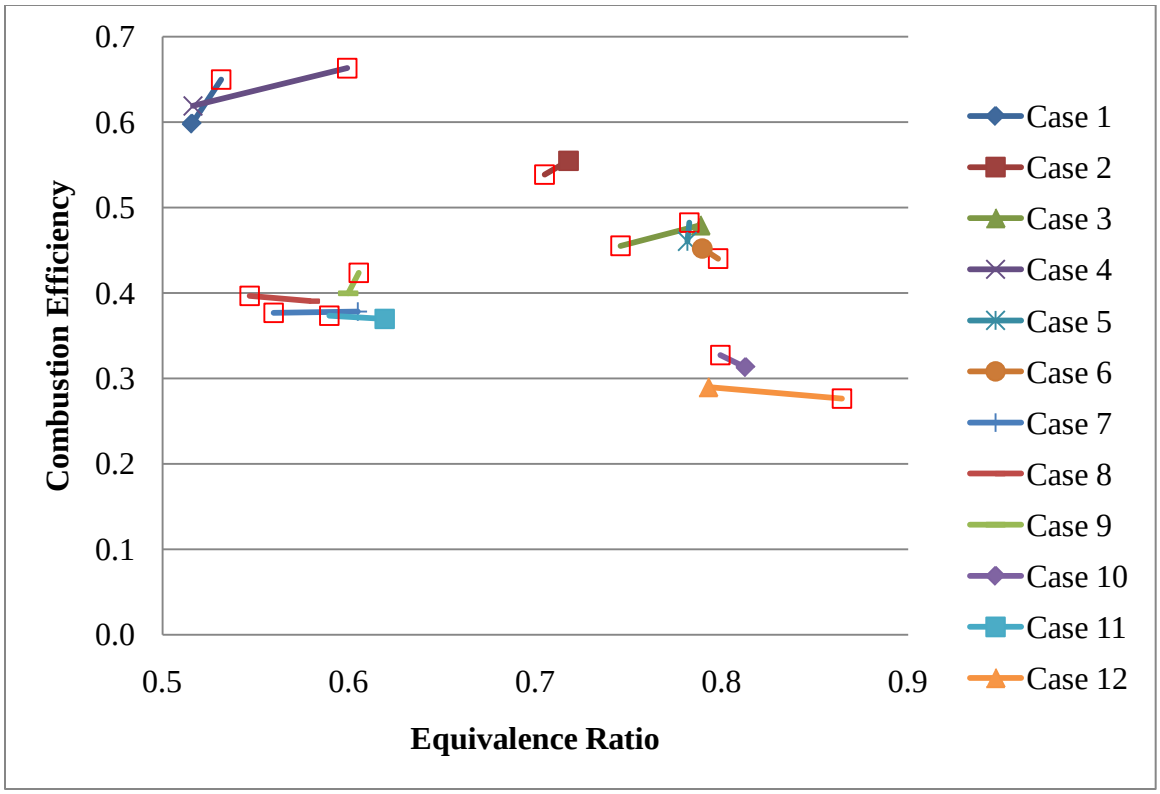


**Figure 26: Combustion efficiency versus total equivalence ratio by case**

The three cases with combustion efficiency above 50% are the only cases analyzed with no downstream fueling. The suggestion is the downstream fuel was not burning well, but the combustion efficiency is calculated correctly. The resulting trend (more fuel added, efficiency gets increasingly lower) also supports the hypothesis of a fuel rich downstream combustion area. The resulting low efficiencies, then, at higher equivalence ratios are reasonable. The four cases with equivalence ratios near 0.6 and efficiencies around 0.4 are the cases where the nominal equivalence ratio is 0.3/0.3 primary/secondary and the Mach 1.8 nozzle was installed. The primary equivalence ratio for these test conditions was near a possible maximum. Figure 27 shows the shock location (as identified by the rapid pressure rise) to be near the inlet. If just a small additional amount of fuel was introduced upstream of the flame holder for the aeroramp

configuration, the result would have been an unstart because the shock train position is very near the start of the isolator (x=0).

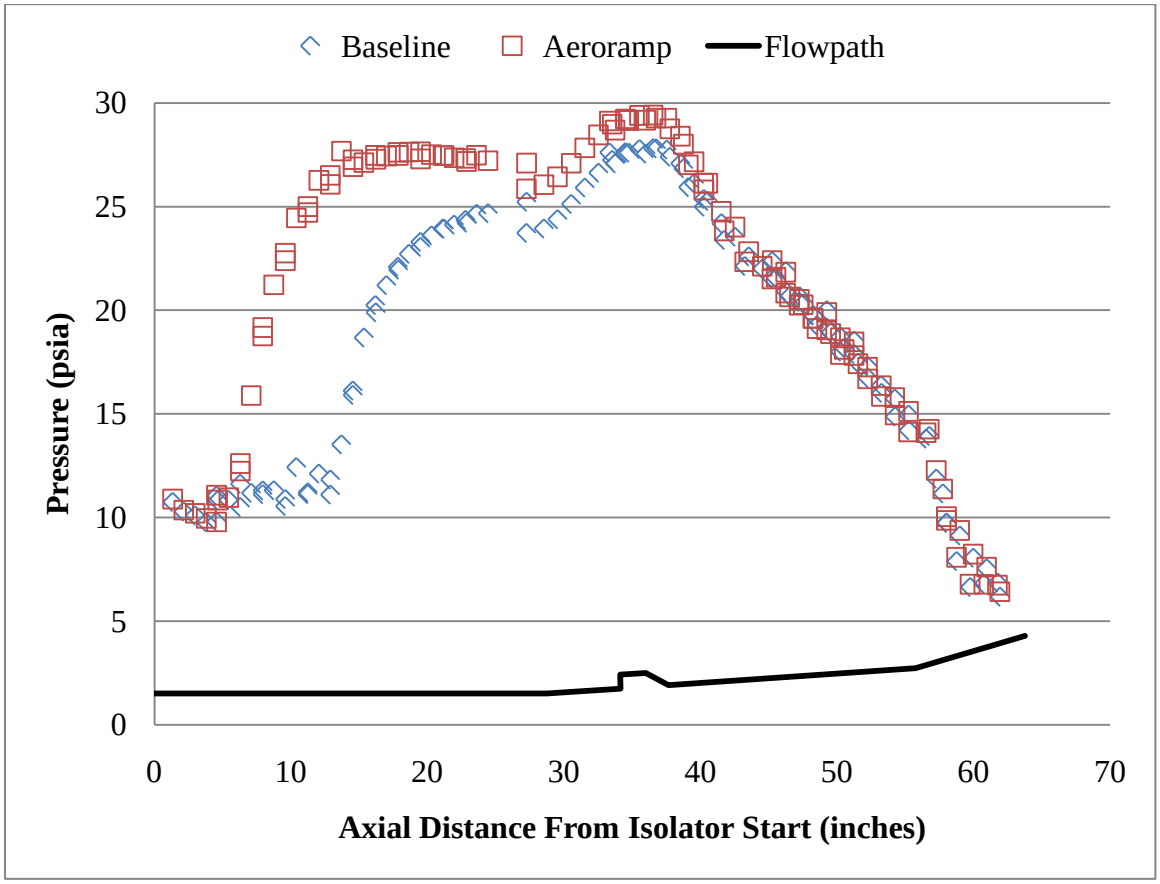


**Figure 27: Wall static pressure for case 9 (m=3.5, q=1000, φ=0.3/0.3)**

The combustion efficiencies from the aeroramp and baseline configurations do not show a clear trend except for the expected decreasing combustion efficiency for increasing equivalence ratio. Figure 28 below shows in some cases the aeroramp has a higher efficiency and some cases the baseline has a higher value, and all but Case 1 are easily within the ~5% error band of the analysis. [16] Therefore, the combustion efficiencies are not statistically, significantly different.

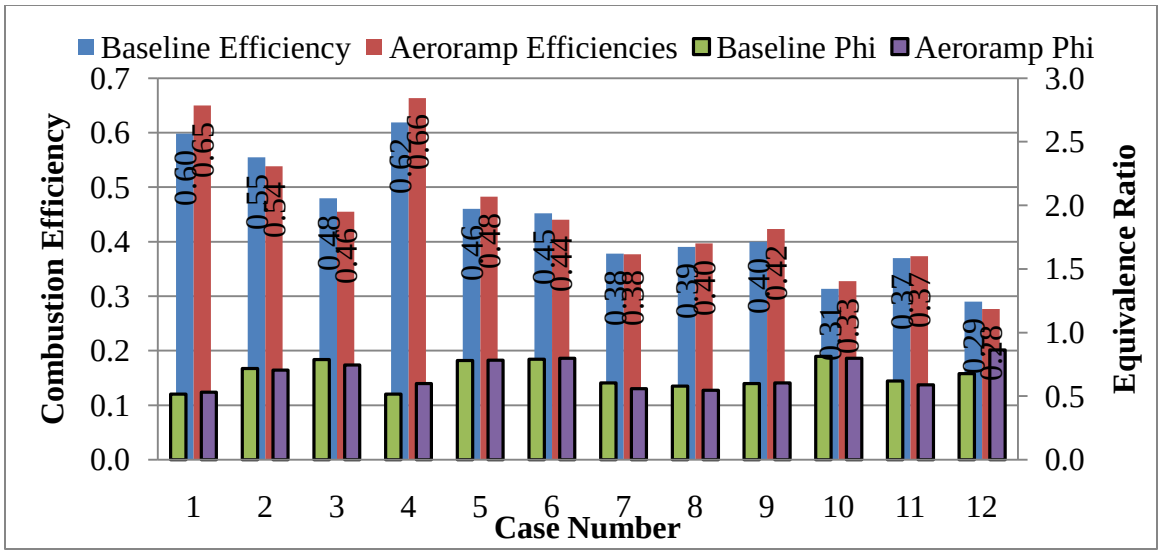


**Figure 28: Combustion efficiency comparison by case**

One potential cause for the similar combustion efficiencies is that the steady-state combustion condition results in a significant portion of the flow being subsonic at the injectors due to the pre-combustion shock train. The effect of the pre-combustion shock on the fuel plume structure of two round 15-degree angled injectors in a cavity–based flame holder can be seen in Figure 29 below for a single hole round injector.

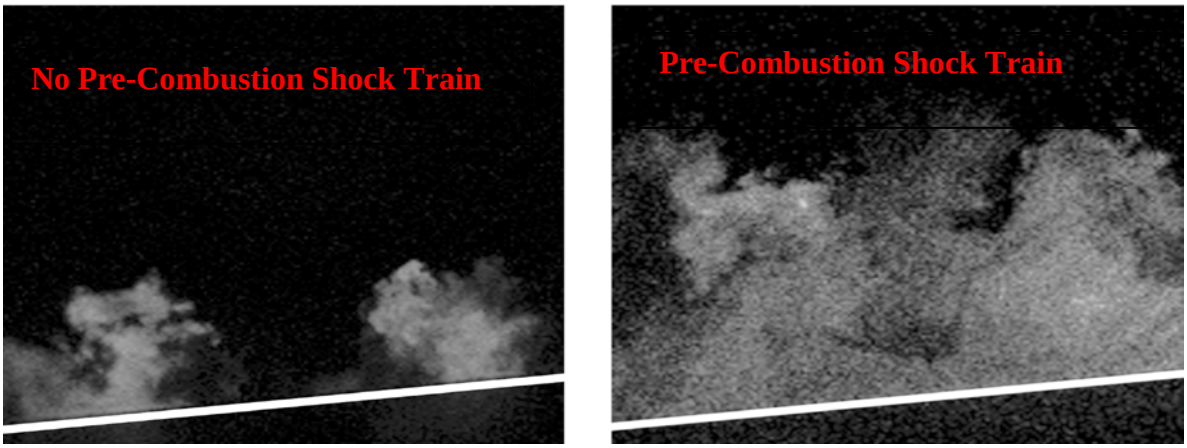


**Figure 29: Instantaneous no PLIF with low/high backpressure (left/right) [17]**

The image on the left corresponds to injection into supersonic flow, the conditions that would exist before combustor ignition, the expected shape from previous work [14].

The image on the right corresponds to injection into the highly distorted flow downstream of a pre-combustion shock train which are the conditions that would exist after combustor ignition. This image shows the plume structure is significantly larger and better mixed. The significant increase in mixing once the combustor is started may make the aeroramp and round injectors both mix similarly. The primary benefit of the aeroramp injector is improved mixing in supersonic flow.

The subsonic flow field would also seem to explain why, at the end of the combustor, the aeroramp and baseline injectors give almost exactly the same wall pressures. If a different amount of fuel had been burned, the aft combustor pressures would have shifted as can be seen in the comparison of the static pressure profiles from the baseline injectors of Case 1 and Case 2 in Figure 30.

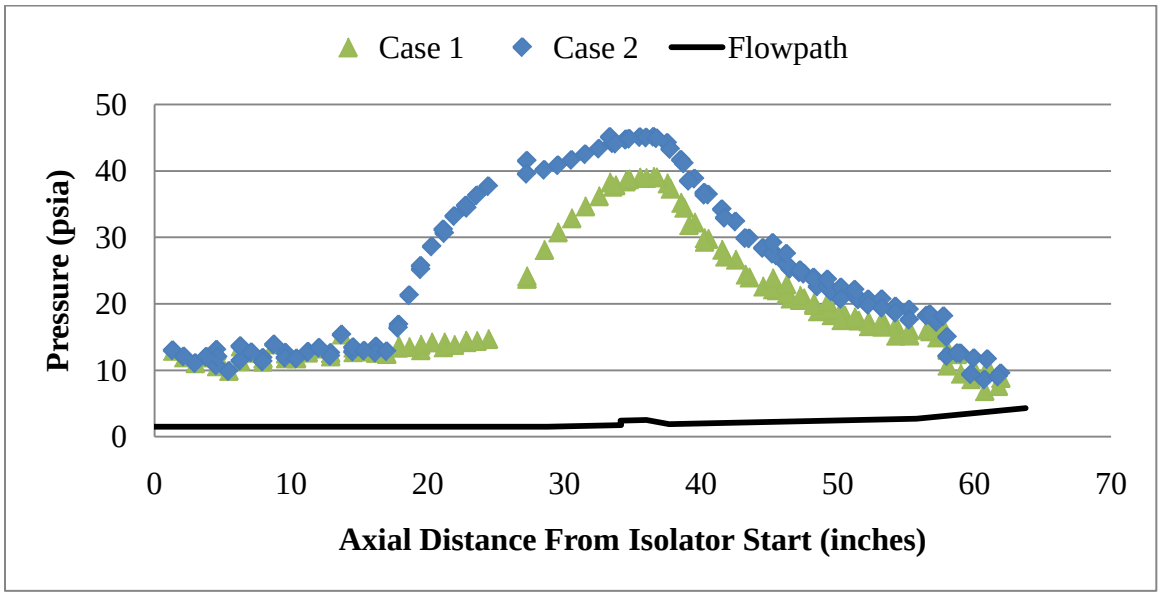


**Figure 30: Axial static pressure profiles for baseline configurations of case 1 and case 2 (m=5, q=1000, φ=0.52 and 0.72)**

The difficulty with this hypothesis is there should not be a change in the shock position or the peak pressure rise. Therefore, the evidence supports the conclusion the

aeroramp does indeed have a larger, better mixed plume. That would allow for the high pressure and temperature combustible fuel/air mixture region of the aeroramp to interact with the combustion radicals from the cavity earlier in the chamber than is the case for the round injectors. This forward movement of the flame front could cause the primary combustion region to occur in the region of the cavity rather than farther aft in the combustor where the area relief is greater. The primary combustion in the cavity region would correspond to the higher peak pressure in the cavity. Although if the same total amount of fuel was combusted, once the area was relieved, the final pressure would gradually trend to be identical. Figure 31 exhibits the pressure trend in the static pressure plot of Case 5 below.

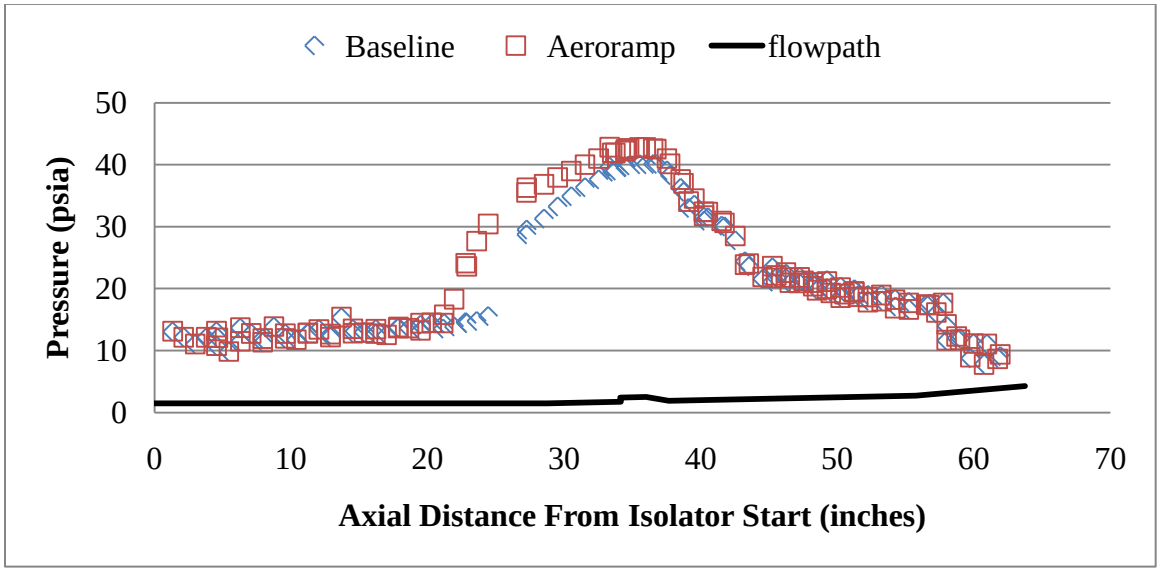


**Figure 31: Axial static pressure profiles for case 5 (m=5, q=1000, φ=0.50/0.28)**

The pressures in the isolator upstream of the precombustion shock match exactly suggesting good run-to-run repeatability. The pre-combustion shock train from the aeroramp arrives earlier. The aeroramp has a higher pressure until near station 40 where they again match exactly. The trend gives credence to the theory of earlier mixing and

combustion, but identical total heat release. Because most of the axial differential area is in the nozzle, it is possible the thrust component of the efficiency and thus the efficiency itself is insensitive to when the combustion occurs.

To determine if there is any effect of the downstream fueling, the efficiency was plotted against the equivalence ratio of the primary fuel injector site in Figure 32 below.

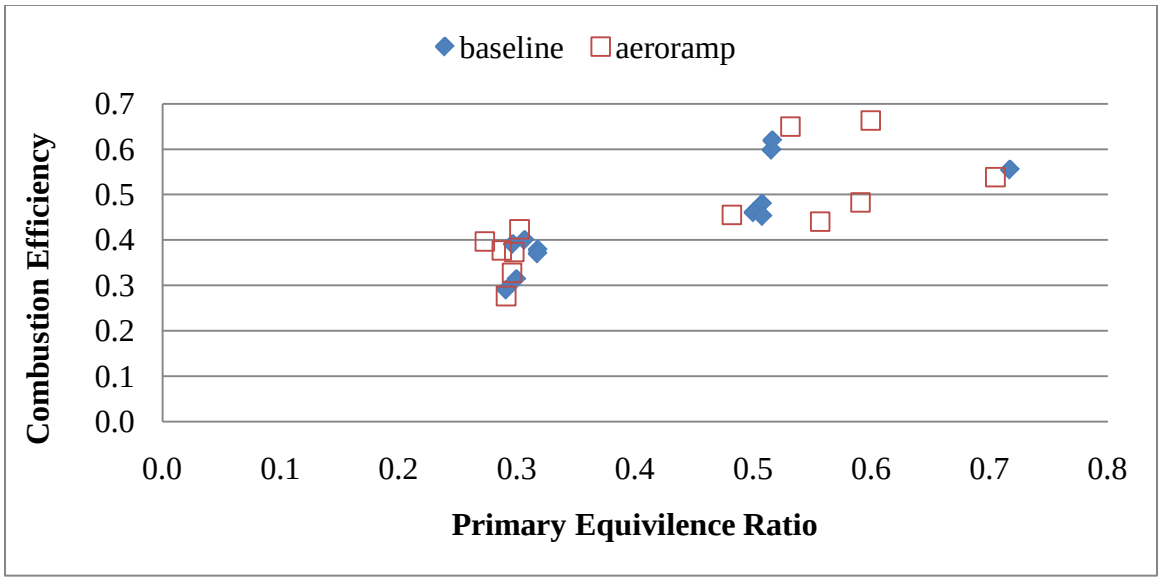


**Figure 32: Combustion efficiency versus primary fuel site equivalence ratio**

The expected trend is that a higher efficiency will result when more of the fuel is injected upstream of the cavity. The data indicates this trend from the slight positive slope between the two sets of data in Figure 32. The lower equivalence ratio cases are for the Mach 1.8 nozzle. The steep but short trend within the Mach 1.8 nozzle grouping shows there is some effect of downstream injection. This is to be expected. At lower Mach numbers, the low maximum equivalence ratio upstream of the flame holder, in this case about 0.30, leaves significant oxygen in the flow for the downstream fuel to mix with and burn.

### *IV.2.2 Stream Thrust*

As a result of the low sensitivity to fuel injectors as indicated by combustion efficiency, other parameters will be used to determine where differences between the aeroramp and baseline occur. While there is no aggregate change in performance, a subtle change can be discovered that when used in a different design has the potential to yield a significant improvement.

Most high sensitivity inputs to combustion efficiency are captured in the stream thrust calculation. Additionally, an improvement in stream thrust alone could justify tolerating a lower efficiency. The sensitivity of stream thrust to equivalence ratio can be seen in Figure 33 below.

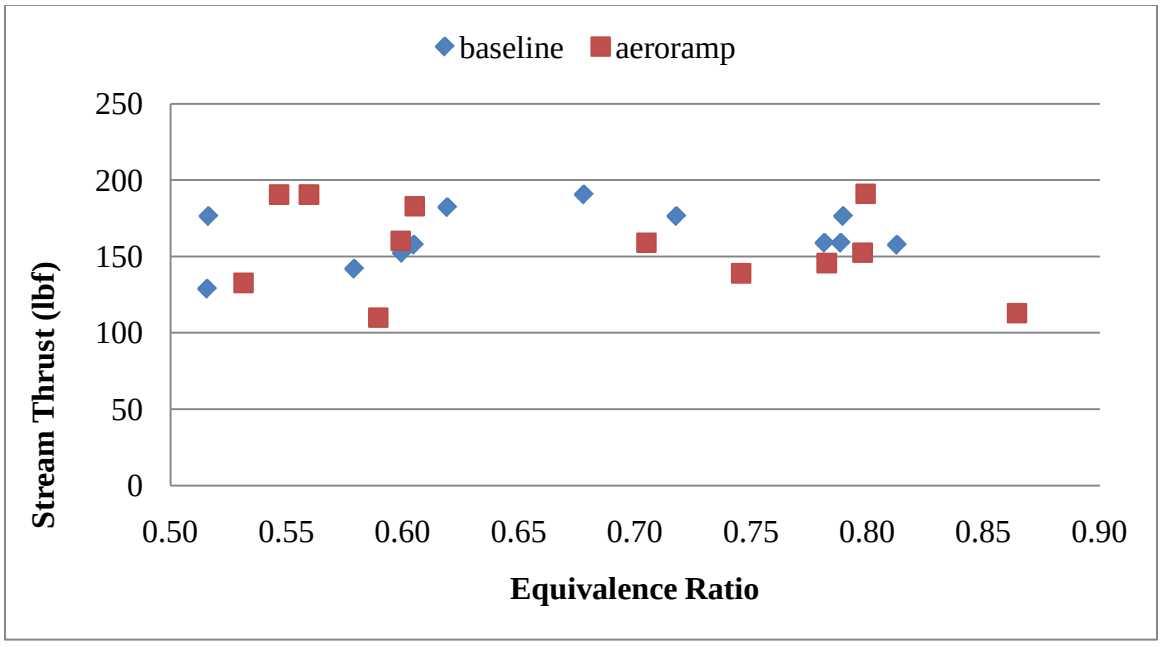


**Figure 33: Non-combusting to combusting stream thrust delta versus total equivalence ratio**

The thrust appears to be relatively constant with respect to both the type of injector and the amount of fuel. The indication is when more fuel is being added, it is not

being burned, directly supporting the hypothesis that the higher equivalence ratios are lower efficiency because the fuel is not being burned. A direct comparison of the thrust between similar conditions can be seen in Figure 34 below.

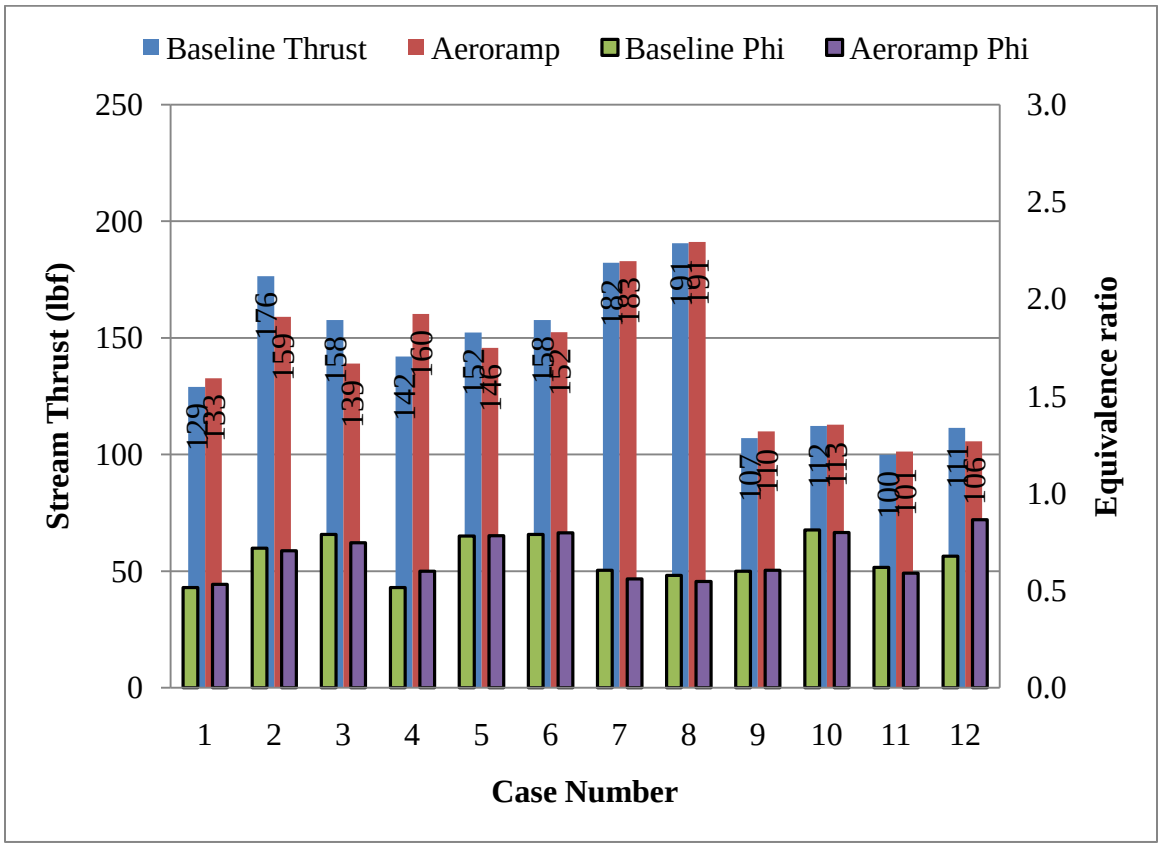


**Figure 34: Combustion stream thrust comparison by case**

The direct comparison also shows there is no significant change in thrust between the aeroramp and baseline configurations. Some of the cases have a higher thrust with the aeroramp. Only some of those have a higher equivalence ratio while some actually have more thrust for less fuel. This comparison indicates the thrust portion of the combustion efficiency is similarly inconclusive in determining any performance changes with the aeroramp injector.

If much of the fuel that is being injected is not being burned, a property that can be examined is the burned equivalence ratio. Based on the definition of combustion efficiency, burned equivalence ratio is simply combustion efficiency multiplied by total equivalence ratio. A plot of stream thrust versus phi burned is seen in Figure 35.

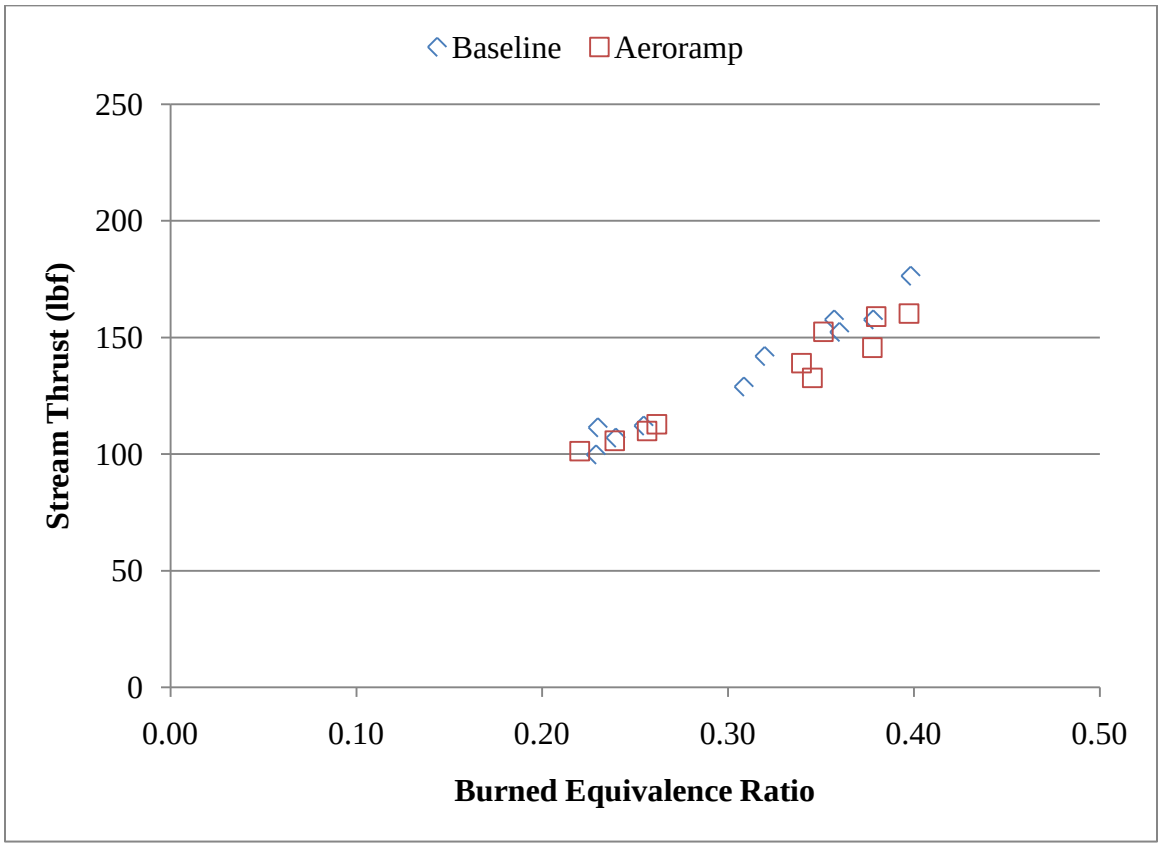


**Figure 35: Stream thrust versus burned equivalence ratio**

There is a very strong trend showing as the actual amount of fuel that is being burned is increased, the thrust increases. The aeroramp configurations appear to be slightly lower in some cases, but only slightly more than the error and not consistently.

### *IV.2.3 Combustor Exit Pressure*

Another parameter that is directly affected by the combustion process is the combustor exit pressure. Exit pressure has a high weight in thrust because the 11-degree divergent truncated nozzle has the bulk of the axial area for the pressure force. For this paper, the combustor exit pressure is calculated as the average of the last two pressure taps in the truncated nozzle: one on the top wall and one on the bottom wall. To allow for comparisons for different inflow conditions, the exit pressure has been normalized by the first isolator pressure tap on the sidewall. The comparison versus equivalence ratio can be seen in Figure 36 below.

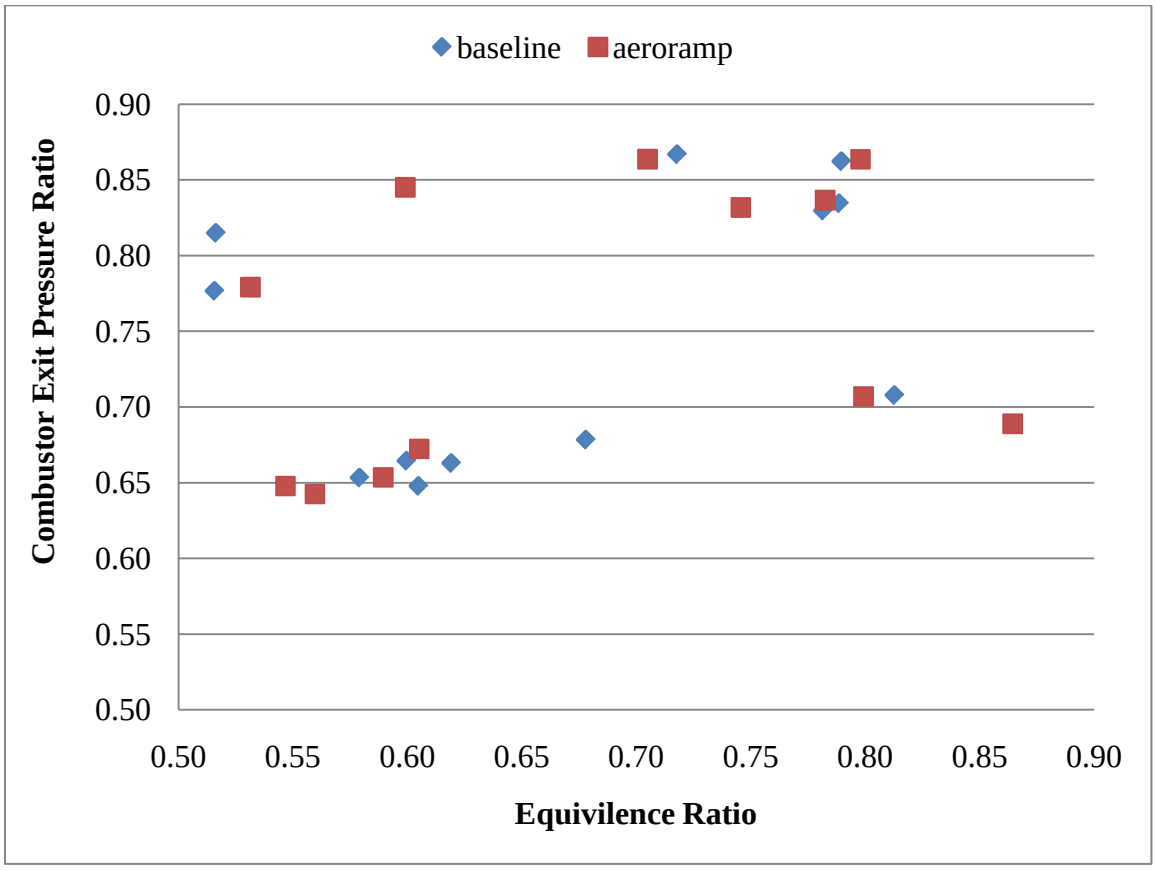


**Figure 36: Combustor exit pressure ratio versus total equivalence ratio**

There are distinct groupings of the data, but they are not separated into aeroramp and baseline or in a global trend for exit pressure ratio. To further understand the trends noticed, the direct comparisons by case are shown in Figure 37 below.

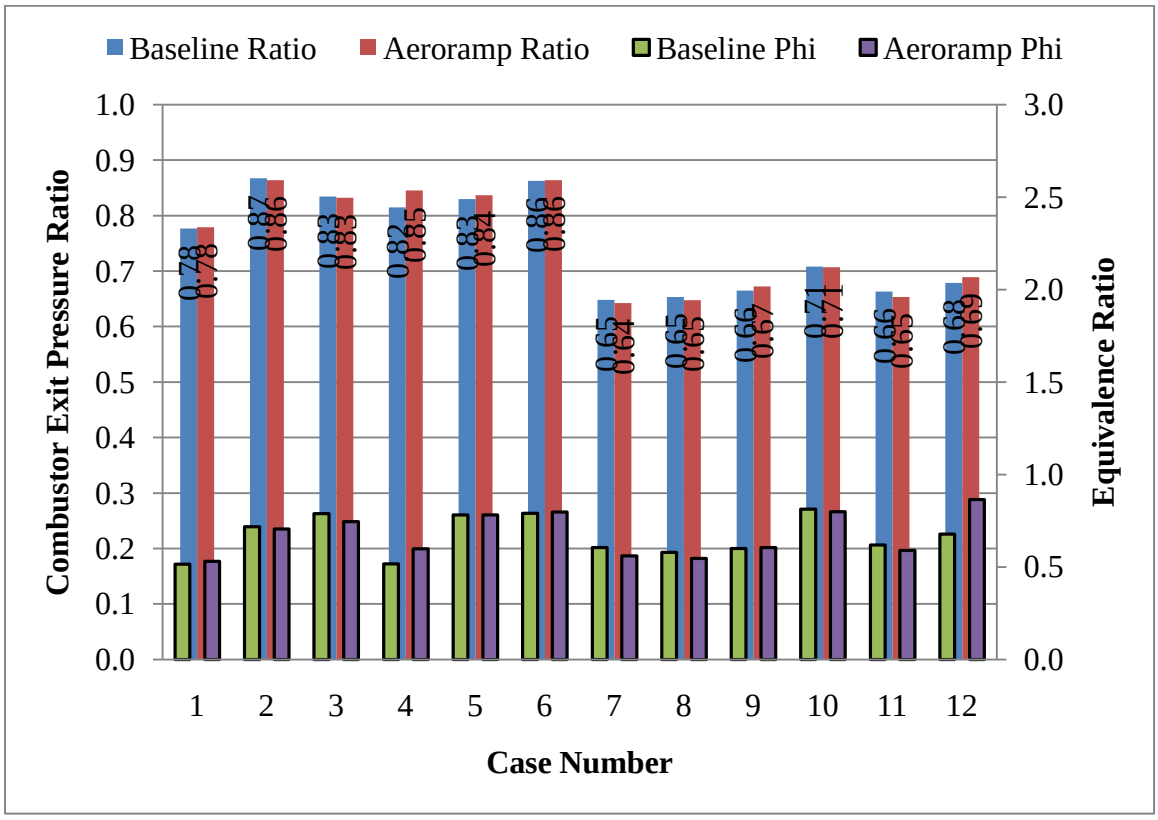


**Figure 37: Combustor exit pressure ratio by case**

The data suggests two trends directly relating to the two different facility nozzles. Cases 1-6 use the Mach 2.2 nozzle and cases 7-12 use the Mach 1.8 nozzle. Within each of these groups, there is no strong sensitivity to injector type. A weak correlation to equivalence ratio is seen in the change from Case 1 to Case 2. The suggestion is increased combustion for these cases, but nothing significantly biased toward one injector over the other. Rather, a higher equivalence ratio corresponded to a higher pressure ratio.

Since the only change is from baseline to aeroramp, a comparison between the combustor exit pressure ratio and the primary equivalence ratio might be useful, Figure 38 below.

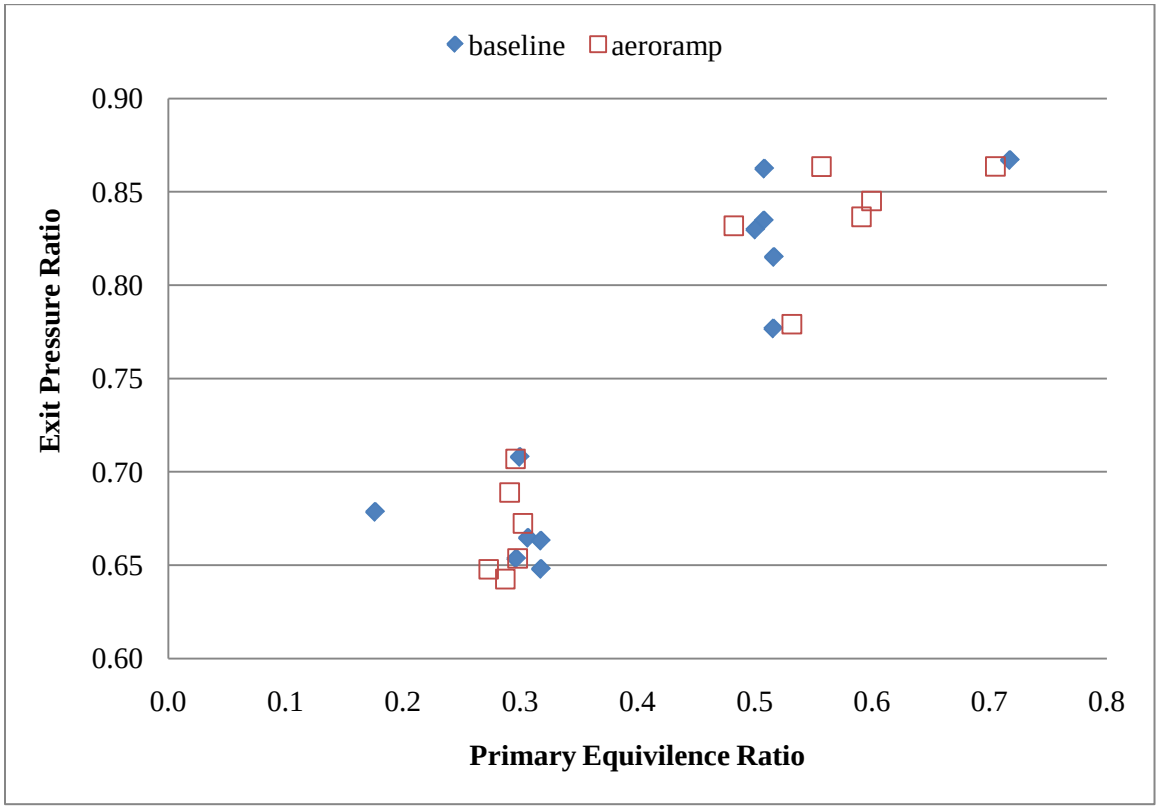


**Figure 38: Exit pressure ratio versus primary equivalence ratio**

The result in Figure 38 suggests a very strong correlation between the exit pressure and the primary equivalence ratio indicated by the rising trend in Figure 38. The vertical relationship at the 0.30 and 0.50 equivalence ratios also suggest another possible influence in the results. The indication is for very similar primary fueling; both the aeroramp and the baseline injector receive a very similar pressure rise from the downstream injection. Additionally, the amount of pressure rise from a given primary fueling condition is consistent between the two types of injectors.

# V. Conclusions and Recommendations

## V.1 Conclusions

The primary areas of interest for this study were the performance and operability implications of replacing four 15 degree round injectors with four arrays of improved aeroramp injectors. The mechanism to determine this was an experimental comparison in a dual-mode scramjet with the two different types of injectors installed at the primary injector site upstream of the flameholder. Ignition limits and pre-combustion shock position were used to define the operability differences while combustion efficiency was the primary metric used for performance comparisons.

Operability was divided into two parts: the range of conditions at which the injectors enabled sustained combustion, and the pre-combustion shock train position within the isolator for the same fuel and air conditions. The baseline fuel injector achieved sustained combustion readily at all simulated Mach numbers (3.5-5) and dynamic pressures (500-2000 psf). The aeroramp injector could not sustain combustion at any Mach number for a dynamic pressure of 500 psf. Combustion could be sustained at 2000 psf using elaborate lighting techniques, but only at a subset of the Mach range. At 1000 psf, the aeroramp could sustain combustion, but required more aerothrottle backpressure before enough combustion pressure was generated to be self sustaining. All conditions where combustion could not be sustained were due to an excessively fuel-rich cavity, even to the point of causing soot deposits on the cavity walls.

Sub-optimal operation could be characterized one of two ways. The first possible cause is the aeroramp injector arrays were not operating properly. The resulting flow

field was four small jets per array unable to penetrate the boundary layer and the fuel was swept into the cavity. A second possibility is the plumes from the arrays of aeroramp injectors interacted more than the round injectors interact and prevented the incoming air from passing between the plumes. The same type of fuel rich cavity behavior would result. Finally, it is also possible the plumes left a fuel rich stem along the wall that, despite favorable mixing in the main flow, made the cavity too rich to ignite.

The ability of the isolator to contain the pressure rise from the combustor upstream of the thermal choke is critical to achieving lower Mach number operation of a dual-mode scramjet. For all fueling conditions where combustion was achieved, the aeroramp injector forced the shock train further forward than the baseline configuration at the same equivalence ratio. The most likely cause is the aeroramp injector did indeed have superior mixing causing the majority of the combustion to occur earlier in the combustor. The resulting enthalpy addition would occur in the forward part of the combustor where the flowpath area is less, thus causing a greater pressure rise. As a result, the pre-combustion shock train moved forward reducing the operability range.

Performance of a scramjet flow path is best compared using the combustion efficiency. For this study, the combustion efficiency differences were generally well within the measurement uncertainty. As a result, the stream thrust and combustor exit pressure ratio were analyzed more closely to shed some light on the performance differences.

All three parameters showed there was no appreciable difference in the performance of the aeroramp injector relative to the baseline injector regardless of the parameter comparison. The anticipated result is the higher pressure rise causing the

reduced operability range would also cause an increase in thrust. This research indicates no additional fuel is being combusted despite the consistently higher maximum pressure ratio of the aeroramp injector. Rather, the experiments seem to merely indicate a more rapid near-field combustion process. Faster combustion is extremely desirable for scramjet mode where there is no pre-combustion shock train, but it does seem to come at a relatively steep operability penalty in dual-mode operation. This result is not entirely unexpected as the original aeroramp designs were designed and tested in a supersonic cross flow. The improved aeroramp was designed for coupling with a plasma torch igniter, which would only be used during startup, before the pre-combustion shock is formed. Further testing was in a Mach 4.0 cross flow, more indicative of the scramjet mode conditions. [18] Operating at scramjet conditions can truly make use of the more rapid plume spreading and mixing of an aeroramp design.

The operability reduces significantly for the aeroramp injector, but the performance is virtually identical to the round injectors. Therefore, the best use of an aeroramp injector in a DMSJ configuration would likely be as an ignition aid and an upstream high Mach fuel injector. The challenge is that there will always be more complicated fabrication, and thus more risk and cost associated with an aeroramp injector, relative to a single, angled wall injector. The implication is the aeroramp should only be considered where the near field mixing of a round injector is insufficient to sustain combustion.

## V.2 Recommendations

There are many opportunities available to further investigate the properties and benefits of an aeroramp style injector. The simplest way is to further analyze the vast data set obtained for this project to include laser-based temperature and water concentration measurements in the truncated nozzle. Another promising study would be to perform 3-D reacting CFD simulations for the aeroramp in a cavity coupled configuration to determine the nature of the fuel plume for a reacting flow. Finally, visualization of the flame front using a technique such as OH- PLIF would verify the conclusions of the CFD.

Only a fraction of the data collected in the test series was analyzed for this research. Many available additional cases that are not direct correlations between the aeroramp and the baseline could be used to investigate the trends in the performance comparisons. These data were not analyzed, as the primary purpose of this research is to directly compare the performance of the aeroramp injector to the round injector.

Additionally, there is a wealth of information recorded using Tunable Diode Laser Absorption Spectroscopy (TDLAS). The TDLAS focused on water concentrations and temperature. The resulting analysis could provide insight into whether there was indeed any additional heat release in the aeroramp cases and show if there is a correlation to a higher peak pressure ratio. The data is currently being processed for analysis but the tool to expedite the analysis will not be available until sometime later in 2009.

The use of CFD to visualize the flow features could be useful in understanding how the aeroramp works and how the operability impacts could be mitigated. A grid exists for the baseline flow path and minor modifications could be made to allow for the analysis of

the aeroramp injector. The primary purpose of the CFD study would be to show how the plumes from the aeroramp injector interact with each other and with the cavity in the presence of a pre-combustion shock train and combustion. The current tools can model this area with high accuracy so the expected results would be very insightful. The ability to understand the cause of the flow to flood the cavity would provide significant benefit to any redesign of the injectors or a design of a combustor utilizing the aeroramp injectors.

Finally, another useful study would be to use a laser diagnostic such as OH-PLIF to determine the location of the flame front. This diagnostic could show whether the combustion is indeed occurring more rapidly with the aeroramp injector as suspected. Additionally, an NO-PLIF could be used in a non-reacting study to better understand the aeroramp mixing environment with elevated backpressure.

## VI. Bibliography


1. Fuchs, Ronald P., Deptula, David A., Chaput, Armand J., Frost, David E. and McMahan, Tom. "Why and Whither of Hypersonics". SAB-TR-00-03. 2000.

2. Hank, Joseph M., Murphy, James S. and Mutzman, Richard C. "The X-51A Scramjet Engine Flight Demonstration Program". AIAA Paper 2008-2540. May 2008.

3. Jacobsen, Lance S, Carter, Campbell D, Jackson, Thomas A, Williams, Skip and Barnett, Jack. "Plasma-Assisted Ignition in Scramjets". AIAA Journal of Propulsion and Power. 2008. Vol. 24, No. 4, pp. 641-654.

4. Price, Bradford B., Elliott, Gregory S. and Ogot, Madara. "Experimental Optimization of Transverse Jet Injector Geometries for Mixing into a Supersonic Flow". AIAA Paper 1998-3019. June 1998.

5. Fuller, Raymond P., Wu, Pei-Kuan, Nejad, Abdollah S and Schetz, Joseph A. "Comparison of Physical and Aerodynamic Ramps as Fuel Injectors in Supersonic Flow". AIAA Journal of Propulsion and Power. 1998. Vol. 14, No. 2, pp. 135-145.

6. Bonanos, Aristides M., Schetz, Joseph A., O'Brien, Walter F. and Goyne, Cristopher P. "Scramjet Operability Range Studies of a Multifuel Integrated Aeroramp Injector/Plasma Ignitor". AIAA Paper 2005-3425. 2005.

7. Jacobsen, Lance S., Gallimore, Scott D., Schetz, Joseph A., O'Brien, Walter F. and Goss, L.P. "Improved Aerodynamic-Ramp Injector in Supersonic Flow". AIAA Journal of Propulsion and Power. 2003. Vol. 19, No. 4, 663-673.

8. Mercier, Robert A. and McClinton, Charles L. "Hypersonic Propulsion - Transforming the Future of Flight". AIAA Paper 2003-2732. July 2003.

9. Baurle, R. A., Fuller, R.P., White, J.A., Chen, T.H., Gruber, M. R. and Nejad, A.S. "An Investigation of Advanced Fuel Injection Schemes for Scramjet Combustion". AIAA Paper 1998-937-939. 1998.

10. Corbin, Christopher R., Wolff, J. Mitch and Eklund, Dean R. "Design and Analysis of a Mach 3 Dual Mode Scramjet Engine". AIAA Paper 2008-2644. April 2008.

11. Mays, R.B., Thomas, R.H. and Shetz, J.A. "Low Angle Injection Into a Supersonic Flow". AIAA Paper 1989-2461. July 1989.

12. Tam, Chung-Jen, Hsu, Kuang-Yu, Gruber, Mark R. and Raffoul, Charbel N. "Fuel/Air Mixing Characteristics of Strut Injections for Scramjet Combustor Applications". AIAA Paper 2008-6925. August 2008.

13. Bonanos, Aristides M., Schetz, Joseph A., O'Brien, Walter F. and Goyne, Cristopher P. "Integrated Aeroramp-Injector/Plasma-Torch Igniter for Methane and Ethylene Fueled Scramjets". AIAA Paper 2006-813. January 2006.

14. Jacobsen, Lance S., Carter, Campbell D. and Dwenger, Andrew C. "Cavity-Based Injector Mixing Experiments for Supersonic Combustors with Implications on Ingiter Placement". AIAA 2006-5268. July 2006.

15. Zucrow, Maurice J. and Hoffman, Joe D. *Gas Dynamics Volume I.* USA : John Wiley & Sons, Inc, 1976. ISBN 0-471-98440-X.

16. Smith, S., Scheid, A, Eklund, D., Gruber, M., Wilkin, H. and Mathur, T. "Supersonic Combustion Research Laboratory Uncertainty Analysis". AIAA Paper 2008-5065. Hartford, CT : s.n., July 2008.

17. Gruber, Mark R., Donbar, Jeff M. and Carter, Campbell D. "Mixing and Combustion Studies Using Cavity-Based Flameholders in a Supersonic Flow". AIAA Journal of Propulsion and Power. 2004. Vol. 20, No. 5, pp. 769-778.

18. Maddalena, Luca, Campioli, Theresa L. and Schetz, Joseph A. "Experimental and Computational Investigation of Light-Gas Injectors in Mach 4.0 Crossflow". AIAA Journal of Propulsion and Power. 2006. Vol. 22, No. 5, pp. 1027-1038.

19. Gallimore, Scott D., Jacobsen, Lance S., O'Brien, W. F. and Schetz, Joseph A. "An Integrated Aeroramp-Injector/Plasma-Igniter for Hydrocarbon Fuels in Supersonic Flow Part B:Experimental Studies of the Operating Conditions". AIAA Paper 2001-1767. April 2001.

20. Gruber, Mark, Carter, Campbell, Ryan, Michael, Rieker, Gregory B., Jeffries, Jay B., Hanson, Ronald K., Liu, Jiwen and Mathur, Tarun. "Laser-Based Measurements of OH, Temperature, and Water Vapor Concetration in a Hydrocarbon-Fueled Scramjet". AIAA Paper 2008-5070. 2008.

21. Jacobsen, Lance S., Gallimore, Scott D., Schetz, Joseph A. and O'Brien, W. F. "Integration of an Aeroramp Injector/Plasma Igniter for Hydrocarbon Scramjets". AIAA Journal of Propulsion and Power. 2003. Vol. 19, No. 2, pp. 170-182.

22. Lin, Kuo-Cheng, Tam, Chung-Jen, Jackson, Kevin, Kennedy, Paul and Behdadnia, Robert. "Experimental Investigations on Simple Variable Geometry for Improving Scramjet Isolator Performance". AIAA Paper 2007-5378. July 2007.

23. Jacobsen, Lance S., Gallimore, Scott D., Schetz, Joseph A., O-Brien, W. F. and Goss, L. P. "An Integrated Aeroramp Injector/Plasma-Igniter for Hydrocarbon Fuels in a Supersonic Flow Part A:Experimental Studies of the Geometric Configuration". AIAA Paper 2001-1776. April 2001.

# VII. Vita

In June of 2001, Dell T. Olmstead graduated from Riverside High School in Chattaroy, Washington. Upon graduating high school, he went on to pursue a Bachelor of Science degree in Aerospace Engineering at Embry-Riddle Aeronautical University in Prescott, Arizona where he was enrolled in the Air Force Reserve Officer Training Corps. Upon completion of his undergraduate studies in May of 2005, he received a commission as a Second Lieutenant in the United States Air Force and his first assignment was at Wright-Patterson Air Force Base working for the Aerospace Propulsion Division of the Air Force Research Lab. In September of 2007, he began graduate studies toward a Master of Science degree in Aeronautical Engineering at the Air Force Institute of Technology. Upon graduation, he will move to Colorado Springs and join the faculty of the United States Air Force Academy Department of Aeronautics.

# REPORT DOCUMENTATION PAGE

*Form Approved*
*OMB No. 074-0188*



| **1. REPORT DATE** *(DD-MM-YYYY)* | **2. REPORT TYPE** | **3. DATES COVERED** *(From – To)* |
|---|---|---|
| 15-06-2009 | Master's Thesis | September 2007 –June 2009 |

**4. TITLE AND SUBTITLE**

Cavity Coupled Aeroramp Injector Combustion Study

**5a. CONTRACT NUMBER**

**5b. GRANT NUMBER**

**5c. PROGRAM ELEMENT NUMBER**

**6. AUTHOR(S)**

Olmstead, Dell T., Captain, USAF

**5d. PROJECT NUMBER**

**5e. TASK NUMBER**

**5f. WORK UNIT NUMBER**

**7. PERFORMING ORGANIZATION NAMES(S) AND ADDRESS(S)**

Air Force Institute of Technology
Graduate School of Engineering and Management (AFIT/EN)
2950 Hobson Way, Building 640
WPAFB OH 45433-8865

**8. PERFORMING ORGANIZATION REPORT NUMBER**

AFIT/GAE/ENY/09-J03

**9. SPONSORING/MONITORING AGENCY NAME(S) AND ADDRESS(ES)**

Aerospace Propulsion Division
Dr. Mark Gruber, (937)255-7350
1950 Fifth Street
Wright-Patterson AFB, OH 45433

**10.SPONSOR/MONITOR'S ACRONYM(S)**
**AFRL/RZA**

**11. SPONSOR/MONITOR'S REPORT NUMBER(S)**

**12. DISTRIBUTION/AVAILABILITY STATEMENT**

APPROVED FOR PUBLIC RELEASE; DISTRIBUTION UNLIMITED.

**13. SUPPLEMENTARY NOTES**

**14. ABSTRACT**

The difficulties with fueling of supersonic combustion ramjet engines with hydrocarbon based fuels presents many challenges that are currently being tackled by the Air Force Research Lab Propulsion Directorate Aerospace Propulsion Division. As the scramjet engine designs are scaled up, the need for a better solution to supersonic mixing has led to the development of many different styles of fuel injection. An aerodynamic ramp injector has been shown to have a quantitative improvement over a physical ramp while still achieving desirable mixing characteristics. The objectives for this research was quantifying the performance and operability implications of replacing four 15 degree round injectors with four arrays of improved aeroramp injectors. Ignition limits and pre-combustion shock position were used to define the operability differences while combustion efficiency was the primary metric used for performance comparisons. Performance and operability data was derived from data taken determining the ignition limits, the wall static pressures, temperature measurements, and thrust stand loading. It was determined that the operability reduces significantly for the aeroramp injector, but the performance is virtually identical to the round injectors. The aeroramp injector indicated improved near-field combustion indicating the potential for better performance in higher Mach number flow to include full scramjet mode.

**15. SUBJECT TERMS**

Scramjet, Supersonic Combustion, Dual Mode Scramjet, Fuel Injection, Aeroramp, Combustion Efficiency

| **16. SECURITY CLASSIFICATION OF:** | | | **17. LIMITATION OF ABSTRACT** | **18. NUMBER OF PAGES** | **19a. NAME OF RESPONSIBLE PERSON** |
|---|---|---|---|---|---|
| **a. REPORT** | **b. ABSTRACT** | **c. THIS PAGE** | | | Richard Branam, Lt Col, USAF |
| **U** | **U** | **U** | **UU** | 76 | **19b. TELEPHONE NUMBER** *(Include area code)* (937) 255-6565, ext 7485 (Richard.Branam@afit.edu) |

**Standard Form 298 (Rev. 8-98)**
Prescribed by ANSI Std. Z39-18